CHAPTER

3

Physical and biogeochemical processes of hyporheic exchange in alluvial rivers

Daniele Tonina[1] *and John M. Buffington*[2]

[1]Center for Ecohydraulics Research, University of Idaho, Boise, ID, United States;
[2]Rocky Mountain Research Station, US Forest Service, Boise, ID, United States

Introduction

Riverine water flows both above the streambed and within the porous sediment surrounding rivers (Nagaoka and Ohgaki, 1990; Mendoza and Zhou, 1992), ubiquitously entering and exiting the permeable streambed and banks as the flow moves downstream (Boano et al., 2014). This interstitial movement of riverine water is called *hyporheic flow* and forms a saturated volume of sediment surrounding alluvial rivers that is termed the *hyporheic zone* (Fig. 3.1A) (Gooseff, 2010). The extent of the hyporheic zone can be defined through biological, geochemical, or hydraulic means and is a transitional area between surface and ground waters. Hyporheic water is primarily stream water (Vaux, 1968) with limited mixing with the ambient groundwater (Hester et al., 2013, 2017). Stream water enters bed and bank sediments in downwelling areas and emerges downstream in upwelling areas (Edwards, 1998) (Fig. 3.1). The downwelling and upwelling fluxes are collectively referred to as *hyporheic exchange,* which stems from a variety of processes (Fig. 3.1C), including (1) spatial variation of hydraulic head along the boundaries of the channel due to flow−topography interactions and changes in channel dimensions, shape, and slope (Thibodeaux and Boyle, 1987; Harvey and Bencala, 1993; Elliott and Brooks, 1997; Boano et al., 2006; Tonina and Buffington, 2007) (Fig. 3.1C1), (2) spatial changes in the lateral and vertical extent of alluvium (Stanford and Ward, 1993; Baxter and Hauer, 2000; Malcolm et al., 2005) (Fig. 3.1C2 and 1C3), (3) spatial changes in the hydraulic conductivity of alluvium resulting from variation in grain size and depositional history (Salehin et al., 2004; Ward et al., 2011; Herzog et al., 2016) (Fig. 3.1C5), (4) flow turbulence that causes pressure fluctuations along the boundaries of the channel and diffusion of momentum into the near-surface sediment (Blois et al., 2014; Grant et al., 2018; Voermans et al., 2018; Roche et al., 2019; Rousseau and Ancey, 2020; Shen et al., 2020)

Groundwater Ecology and Evolution, *Second Edition*
https://doi.org/10.1016/B978-0-12-819119-4.15001-2

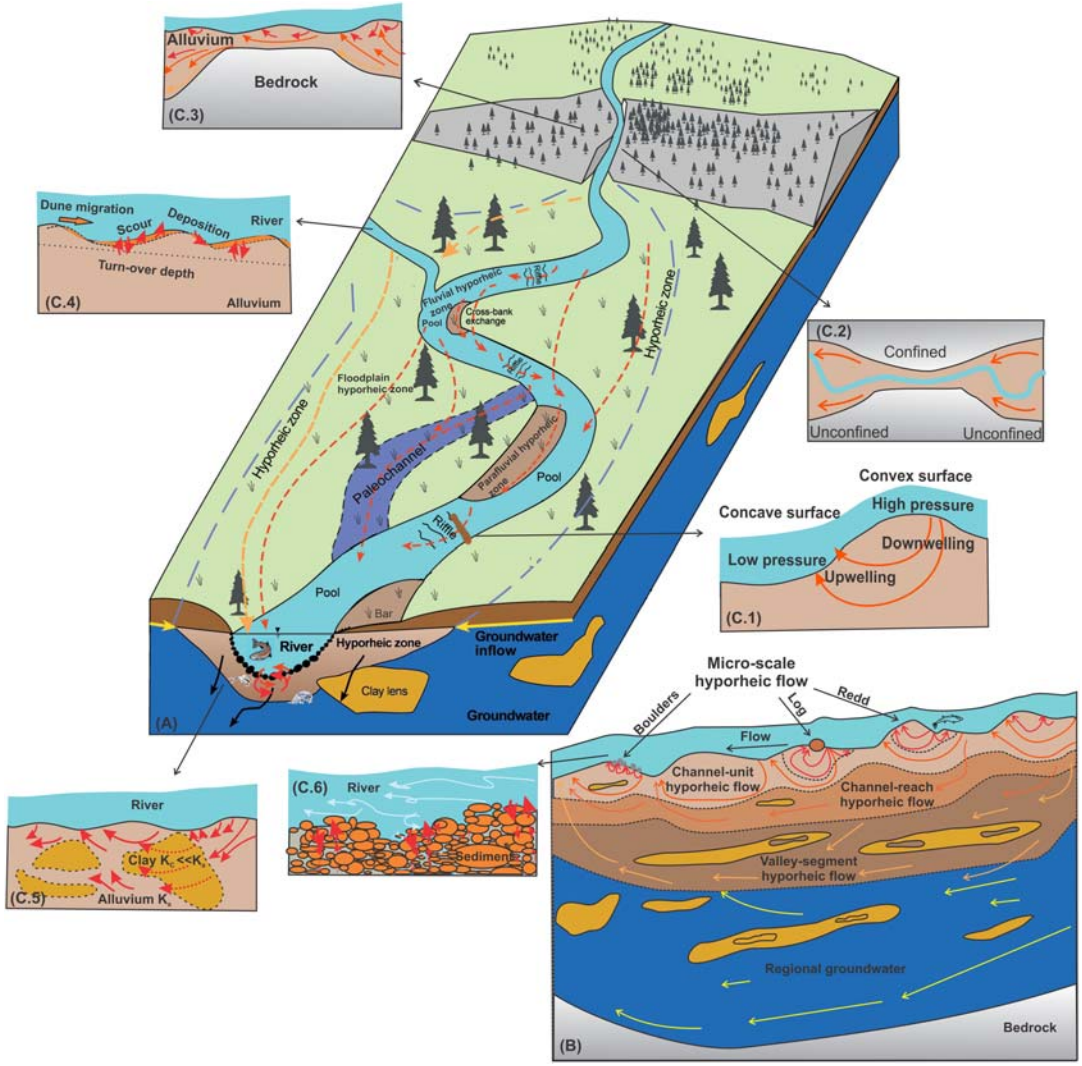

FIGURE 3.1 Surface, hyporheic, and groundwater flow domains in an alluvial valley (A) showing a variety of hyporheic flow paths that move river water into the surrounding porous alluvium and back again (dashed lines from red to orange illustrating micro to valley hyporheic flows), a process termed *hyporheic exchange*. The spatial extent of this exchange defines the *hyporheic zone*, which can be subdivided into hyporheic flow within the channel (*fluvial hyporheic zone*), below exposed bars surfaces (*parafluvial hyporheic zone*), and through buried paleochannels and between meander bends (*floodplain hyporheic zone*) (A). Hyporheic flow is characterized by nested circulation cells (B, red to orange arrows) driven by successive scales of topography, ranging from small-scale objects in the streamflow (e.g., logs, boulders, biotic mounds), to individual meso-scale bedforms, to reach-scale repeating sequences of bedforms (e.g., pool-riffle morphology), and to valley-scale undulations in subsurface bedrock topography, with correspondingly greater mean residence times (from seconds to years) of exchange for longer flow paths. Hyporheic exchange is distinguished from far-field inflow of groundwater (A and B, yellow arrows) and from one-way outflow of river water (i.e., flow paths that do not circulate water from the river and back again). Horizontal and vertical components of regional groundwater flow further modulate the extent of the hyporheic zone (A and B, yellow arrows). Major mechanisms inducing hyporheic exchange are spatial variation of hydraulic head along the boundaries of the channel due to flow−topography interactions (C1), spatial variation in alluvial area due to lateral changes in valley confinement (C2) and vertical changes in alluvial depth driven by underlying bedrock topography (C3), sediment transport and bedform migration (*turnover exchange*) (C4), spatial variation in hydraulic conductivity of the sediment due to changes in grain size and depositional history (C5), and near-bed turbulence causing pressure fluctuations and diffusion of momentum into the near-surface sediment (C6). *Modified from Buffington and Tonina (2009) and Tonina and Buffington (2009), based on drawings by White (1993), Gibert et al. (1994), Harvey et al. (1996), Edwards (1998), Alley et al. (1999), Baxter and Hauer (2000), Dent et al. (2001), Malard et al. (2002), and Stanford (2006).*

(Fig. 3.1C6), (5) density differences between surface and pore waters due to differences in water temperature and chemistry (Boano et al., 2009), and (6) bedload transport that induces bedform migration in sand-bed rivers (Wolke et al., 2019) such that pore water is released from the eroded sediment and stream water is entrained within the deposited sediment; a phenomenon termed *turnover exchange* (Elliott and Brooks, 1997) (Fig. 3.1C4). The relative importance of these mechanisms of hyporheic exchange depends on stream geometry, discharge, and channel type, which vary along the stream network primarily as a function of slope and drainage area (Buffington and Tonina, 2009; Wondzell and Gooseff, 2013; Magliozzi et al., 2018). Furthermore, hyporheic flow typically exhibits nested scales of circulation cells driven by successive scales of topography, ranging from small-scale objects in the streamflow (e.g., boulders, logs, biotic mounds), to individual meso-scale bedforms (e.g., dunes), to reach-scale sequences of repeating bedforms (e.g., pool-riffle or step-pool morphology), and finally to valley-scale undulations of subsurface bedrock topography (Edwards, 1998; Baxter and Hauer, 2000; Dent et al., 2001; Malard et al., 2002; Poole et al., 2008; Buffington and Tonina, 2009; Stonedahl et al., 2013) (Fig. 3.1B). Similarly, nested scales of circulation occur in plan-view due to hyporheic exchange within the wetted channel (*fluvial hyporheic zone*), below exposed bars surfaces (*parafluvial hyporheic zone*), and through buried paleochannels and between meander bends (*floodplain hyporheic zone*) (Fig. 3.1A). These nested circulation cells are conceptualized in vertical and horizontal domains, but are actually complex three-dimensional flow fields. The vertical (basal) and horizontal (underflow) components of ambient groundwater flow further modulate hyporheic flows, their width and depth, *residence time* (the time stream water spends in the sediment), and discharge (Cardenas and Wilson, 2007b; Boano et al., 2008; Cardenas, 2009a; Fox et al., 2014) (Fig. 3.1A and B). Thus, both vertical and horizontal extents of the hyporheic zone vary spatially due to changes in stream and valley size, channel morphology, sediment characteristics, and temporally due to changes in water-table height, groundwater flow, fluvial discharge, sediment transport, and evolution of channel topography (Fig. 3.1) (Stanford and Ward, 1993; Malard et al., 2002; Stanford, 2006; Buffington and Tonina, 2009; Magliozzi et al., 2018). Hyporheic exchange can be predicted for different channel morphologies and across a range of spatial scales, each of which is characterized by different rates and magnitudes of exchange.

Hyporheic exchange also influences water quality by bringing surface water laden with solutes and suspended particles into sediment interstices (Ren and Packman, 2004a; Harvey et al., 2012; Drummond et al., 2014), where reactive solutes undergo biogeochemical transformations due to biofilms attached to streambed particles or are taken up by organisms dwelling within particle interstices (Janssen et al., 2005) (Fig. 3.2). Products of such transformations are then carried away by hyporheic flows (Bott et al., 1984; Triska et al., 1993) and brought to the surface water by upwelling fluxes (Triska et al., 1989a; Nagaoka and Ohgaki, 1990; Mulholland et al., 2008). These transformations depend on reaction time, water temperature, solute concentrations, flow velocity, and length of the hyporheic flow path (Findlay et al., 1993; Ocampo et al., 2006), all of which are stream-size dependent. In small and intermediate streams (<30 m wide), population densities of microorganisms are higher in the hyporheic zone than in the water column, such that most microbially mediated transformations occur in the hyporheic zone rather than in the water column (Wuhrmann, 1972; Master et al., 2005; Marzadri et al., 2017). In this chapter, we describe operative definitions of the hyporheic zone, models for predicting hyporheic exchange in different channel types and across different spatial scales, and finally the role of hyporheic exchange in water quality.

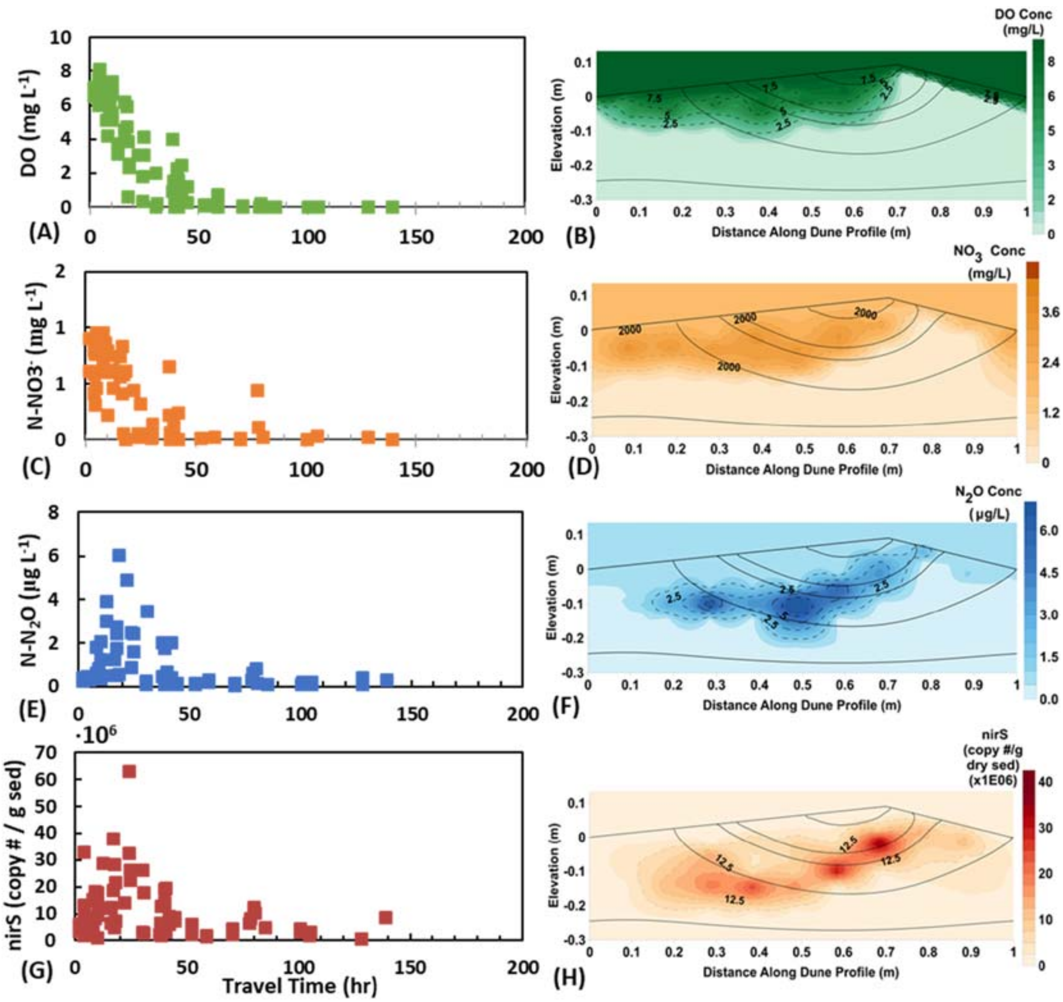

FIGURE 3.2 Trends of dissolved oxygen (DO) (A), nitrate (NO_3^-) (C) and nitrous oxide (N_2O) concentrations (E) and abundance of microbial nitrate reductase genes (nirS) associated with denitrifying environments (G) as a function of travel time within the hyporheic zone induced by dune bedforms (9 cm high × 100 cm long) in a laboratory flume. Spatial distributions of each constituent within the dune are respectively shown in (B), (D), (F), and (H), with surface flow from left to right. Solid black lines in (B), (D), (F), and (H) show subsurface hyporheic flow and groundwater flow (lowest flow line). *Modified from* Quick et al. (2016) *and* Reeder et al. (2018a, 2019).

The hyporheic zone

The hyporheic zone has been traditionally identified via three operational approaches: biological, geochemical, and hydraulic. The hyporheic zone was first studied by biologists because of its function in carrying oxygen-rich stream waters to salmonid embryos incubating in streambed nests called redds (Stuart, 1954). Subsequently, the identification of a characteristic group of macroinvertebrates, termed *hyporheos*, which were neither benthos nor groundwater fauna (Orghidan, 1959), led to the identification of the hyporheic zone as an ecotone whose extent was delineated by the presence or absence of hyporheos (Edwards, 1998).

In contrast, the geochemical method for defining the hyporheic zone uses the chemical signature of surface water, which is different from that of the ambient groundwater. The approach defines the hyporheic zone as the volume of sediment containing an arbitrary amount of surface water (e.g., 10%) (Triska et al., 1989a; Singh et al., 2020). The selected constituent for geochemical differentiation could be a natural component of the fluid, such as pH, radon (Cranswick et al., 2014), or water temperature (Hatch et al., 2006; Constantz, 2008), or it could be an introduced tracer, such as fluorescein, rhodamine, and various types of chlorides, added to the surface flow (Bencala and Walters, 1983; Castro and Hornberger, 1991; Gooseff and McGlynn, 2005; Ward et al., 2010). Recently, the use of "smart" tracers, which are biologically sensitive, like resazurin that irreversibly transforms to resorufin in the presence of aerobic microbial communities (Haggerty et al. 2009; Argerich et al., 2011; González-Pinzón et al., 2012) help in quantifying the aerobically reactive portion of the hyporheic zone (Briggs et al., 2013; Knapp et al., 2017). Selected constituent concentrations can be measured within the sediments with an array of sampling devices placed within the channel and the surrounding floodplain (Wondzell and Swanson, 1996; Gariglio et al., 2013) from which three-dimensional maps of the hyporheic zone can be generated (Harvey et al., 1996).

Finally, the hydraulic method delineates the hyporheic zone as the assemblage of all downwelling flowlines that reemerge in downstream upwelling areas over a given spatial scale of analysis and are predicted with coupled surface-subsurface hydraulic models (Cardenas and Zlotnik, 2003; Lautz and Siegel, 2006) or quantified from measured piezometric heads in field and flume studies (Winter et al., 1998; Storey et al., 2003).

Whereas the three methods can provide different boundaries due to spatial and temporal changes in physicochemical conditions (e.g., discharge, solute concentration, and water table levels), they all identify the unique characteristic of the hyporheic zone as a transitional area between surface and ground waters. In contrast to early studies, which suggested that the hyporheic zone is a mixing area between surface and subsurface water (i.e., groundwater) (e.g., Edwards, 1998), recent investigations highlighted that the hyporheic zone is surface water only, whose physicochemical signature changes with residence time within the alluvium (Gooseff, 2010), and with limited mixing with the surrounding groundwater (Hester et al., 2013, 2017).

Predicting hyporheic exchange

Any object, e.g., ripples (Marion et al., 2002), dunes (Elliott and Brooks, 1997), protruding particles (Hutchinson and Webster, 1998; Dudunake et al., 2020), animal and plant mounds (Cooper, 1965; Ziebis et al., 1996; Yuan et al., 2021; Moreto et al., 2022), boulder steps (Hassan et al., 2015), logs (Sawyer et al., 2011), and beaver dams (Briggs et al., 2012), placed in the streamflow will induce a pressure distribution from spatial changes in flow depth and bed elevation (piezometric head) and/or flow velocity (dynamic head), driving local hyporheic downwelling and upwelling, referred to as *pumping exchange*. Similarly, changes in flow direction within channel bends (Cardenas and Zlotnik, 2003) and other sinuous flow paths (Boano et al., 2010a) can induce pressure distributions that form hyporheic flows across the streambed and banks. These mechanisms may be superimposed on one another, i.e., a set of ripples could be on top of a dune within a meandering channel (Stonedahl et al., 2010), forming a nested series of hyporheic flow paths with different spatial scales (Fig. 3.1B). Hyporheic exchange models have been developed for select bedforms and macro-roughness elements at the bedform (Elliott and Brooks, 1997), reach (Wörman et al., 2002; Lautz and Siegel, 2006; Gooseff et al., 2007; Zarnetske et al., 2008), and landscape (Wörman et al., 2006; Stewart et al., 2011; Gomez-Velez and Harvey, 2014) scales.

Bedform scale

At the bedform scale, Elliott and Brooks (1997) proposed the first Darcy-based "pumping" model for predicting pressure-driven hyporheic exchange in sand-bedded channels with two-dimensional dune-like bedforms. The near-bed head, h, was modeled as a regular sinusoidal distribution reflecting periodic drops in pressure due to bedform drag and turbulent energy dissipation along the length of the bedform (Vittal et al., 1977; Shen et al., 1990)

$$h = h_m \sin\left(\frac{2\pi}{\lambda} x\right) \tag{3.1}$$

$$h_m = 0.28 \frac{U^2}{2g} \begin{cases} (0.34Y^*)^{-3/8}, & Y^{*-1} \le 0.34 \\ (0.34Y^*)^{-3/2}, & Y^{*-1} > 0.34 \end{cases} \tag{3.2}$$

where h_m is the amplitude of near-bed head variation over the bedform, x is the longitudinal distance, U is the mean flow velocity, g is the gravitational acceleration, Y^* is the dimensionless water depth, defined as the ratio between Y_0, the mean hydraulic flow depth, and Δ, the bedform amplitude, and λ is the bedform length. The constant 0.28 is also a function of Y^* (Vittal et al., 1977; Fox et al., 2014), which may lead to a certain degree of error when applied beyond the experimental conditions of Shen et al. (1990). The spatially averaged hyporheic flux, $\overline{q}$, through a dune with homogeneous hydraulic conductivity, K_c, and a basal (vertical) groundwater flow, v_{gw}, at a given alluvial depth, d_b, can be quantified as (Boano et al., 2008; Marzadri et al., 2016)

$$\begin{cases} \overline{q}_{H,G} = \dfrac{u_m}{\pi}\sqrt{1 - \dfrac{v_{gw}^2}{u_m^2}} - \dfrac{v_{gw}}{\pi} \arccos\left(\dfrac{v_{gw}}{u_m}\right) \\ \overline{q}_{H,L} = \dfrac{u_m}{\pi}\sqrt{1 - \dfrac{v_{gw}^2}{u_m^2}} - \dfrac{v_{gw}}{\pi} \arccos\left(\dfrac{v_{gw}}{u_m}\right) + v_{gw} \end{cases} \tag{3.3}$$

$$u_m = K_C \lambda h_m \tanh(\lambda d_b) \tag{3.4}$$

where $\overline{q}_{H,G}$ and $\overline{q}_{H,L}$ are the mean hyporheic fluxes for gaining and loosing reaches, respectively, and u_m is the maximum downwelling velocity. Analytical solutions of the above equations demonstrate that the groundwater underflow (horizontal) velocity, u_{gw}, does not affect the magnitude of hyporheic exchange, but does influence its extent and residence time (Boano et al., 2008; Fox et al., 2014; Marzadri et al., 2016). However, the vertical component of groundwater flow, v_{gw}, strongly impacts the hyporheic exchange, such that the hyporheic zone is fully suppressed for $v_{gw} > u_m$ in Eq. (3.3) (Marzadri et al., 2016). Predictions from these equations have been confirmed by flume experiments, which mimicked ambient groundwater flows (Fox et al., 2014). The residence time distribution $\overline{R}$ of hyporheic flow weighted over the downwelling flux across a dune can be estimated by the following implicit equation as a function of time, t, and sediment porosity, n, for the case of $v_{gw} = 0$

$$\frac{4\pi^2 K_C h_m t}{\lambda^2 n} = \frac{2a \cos(\overline{R}) \tanh\left(\frac{2\pi}{\lambda} d_b\right)}{\overline{R}} \tag{3.5}$$

and semianalytical solutions, which account for ambient groundwater flow, are also available (Bottacin-Busolin and Marion, 2010; Marzadri et al., 2016). In all cases, a lognormal distribution provides a good approximation of $\overline{R}$ (Wörman et al., 2002; Marzadri et al., 2016), although it has been suggested that its accuracy is less reliable in describing the tail of the distribution (Haggerty et al., 2002; Cardenas, 2007) and other distributions have been proposed (Grant et al., 2020). The vertical depth of hyporheic exchange, d_h, when not confined by a finite depth of alluvium, d_b, scales with bedform length, with $d_h \sim 1\ \lambda$ (Wörman et al., 2002), and also depends on the Reynolds number calculated from the mean velocity at the bedform crest, Δ (Cardenas and Wilson, 2007b). The above results for two-dimensional dunes can be used to approximate those of three-dimensional dunes, especially at high Reynolds numbers (Chen et al., 2015, 2018).

Typically, dunes are not stationary, but migrate at a downstream velocity, U_b, causing progressive turnover of the sediment, which simultaneously releases and entraps hyporheic fluid (Fig. 3.2D). The dimensionless turnover number is (Elliott and Brooks, 1997)

$$T_{over} = \frac{nU_b - u_{gw}}{u_m} \tag{3.6}$$

and can be used to estimate the relative dominance of pumping exchange ($T_{over}<0.5$) vs. turnover exchange ($T_{over}>7$) (Elliott and Brooks, 1997), where U_b is multiplied by sediment porosity, n, to create a pore-water velocity of the same type as the Darcy velocities u_{gw} and u_m. For turnover exchange ($T_{over}>7$), the mean downwelling flux can be quantified as

$$\overline{q} = \frac{Y_0}{\lambda} nU_b \tag{3.7}$$

The maximum d_h for turnover exchange was originally suggested to be limited by the amplitude of the largest migrating dune (Elliott, 1990), such that rapid dune migration reduces the depth of hyporheic exchange, which scales with Δ, compared to the case of pumping exchange, where d_h scales with λ. Subsequently, it has been proposed that turnover is always impacted by pumping, which advectively moves solute from the well-mixed turnover region to the subsurface sediment, effectively increasing the depth of hyporheic exchange (Packman and Brooks, 2001).

The original Elliott and Brooks model has been expanded for unsteady surface discharge (Boano et al., 2007b; 2010b), for horizontally stratified streambeds having different hydraulic conductivity (Marion et al., 2008a), and for the effects of colloid deposition within the hyporheic zone (Packman et al., 2000; Ren and Packman, 2004b, 2007). In addition to these analytical solutions, numerical simulations also have been used by coupling surface and groundwater models in fluvial (Cardenas and Wilson, 2007a; Janssen et al., 2012) and marine (Cardenas et al., 2008) dunes. Dune morphology quickly adapts to the applied discharge as sand is typically mobile, even at low flows. This suggests that analysis of hyporheic exchange in sand-bed rivers should account for the dependence of dune size on discharge (Boano et al., 2013). For instance, dune height and length in equilibrium with the stream flow can be assumed equal to 0.167 and 6 times Y_0, respectively (Yalin, 1964). Furthermore, sand-bed rivers can exhibit a broad range of bed topography that varies systematically with discharge and bed load transport rate, transitioning from plane-bed to ripples to dunes and antidunes (e.g., Middleton and Southard, 1984), creating complex spatiotemporal changes in hyporheic exchange.

Most solutions for hyporheic flow through dunes have been quantified assuming that hydraulic conductivity, K_c, is homogenous (same value throughout the domain) and isotropic (same value in all directions). For such conditions, K_c can be estimated as a function of a reference grain size, for instance the median grain size d_{50} (m) (Salarashayeri and Siosemarde, 2012; Gomez-Velez et al., 2015),

$$K_c = 119.06 d_{50}^{1.62} \tag{3.8}$$

Homogeneous and isotropic K_c values yield regular, smoothly varying hyporheic flow paths. In contrast, sediment heterogeneity (i.e., spatially variable K_c) leads to a seemingly erratic distribution of the interstitial flow field (Hester et al., 2013) and generates hyporheic exchange fluxes due to conservation of mass, causing the velocity and direction of subsurface flow to diverge due to spatial changes in sediment porosity (Vaux, 1968; Ward et al., 2011). The phenomenon can manifest at two distinct scales: (1) that of a single textural facies (continuous heterogeneity) (Hester et al., 2013), which is the intrinsic heterogeneity of a given porous material (e.g., sand) due to random spatial changes in grain size and porosity within a given medium and (2) that of multiple, juxtaposing, textural facies at larger spatial scales (categorical heterogeneity) (Winter and Tartakovsky, 2002; Riva et al., 2006; Pryshlak et al., 2015), forming a composite porous medium (e.g., sand and gravel layers, interspersed with clay lenses).

Recent investigations for typical degrees of continuous heterogeneity of hydraulic conductivity in sand-bed streams (standard deviation of the log transformed K_c, i.e., $\sigma_Y^2 < 0.6$, where $Y = ln(K_c)$), show that hyporheic exchange statistics at the bedform scale (e.g., residence time and mean fluxes) can be reasonably approximated using homogeneous K_c values (Tonina et al., 2016). Heterogeneity causes the hyporheic zone to be compressed toward the stream-water interface and an increase in tortuosity of hyporheic flow lines. The former effect reduces the length of the long flow lines (and their residence times), while the latter effect increases the length (and thus the residence times) of the short flow lines with respect to the case of homogeneous hydraulic conductivity. Because the hyporheic zone is strongly dominated by boundary conditions, especially the pressure profile at the water–sediment interface, heterogeneity may reduce the ensemble means of the hyporheic flow (e.g., residence time and fluxes) (Tonina et al., 2016) or increase them (Laube et al., 2018), depending on surface morphodynamic conditions and the consequent pressure distribution at the water–sediment interface. Anisotropy tends to reduce the uncertainty around the ensemble value, namely the difference in flow paths among all the possible heterogeneous realizations of the K_c-field. Investigations of categorical heterogeneity (flow through multiple textural facies) show similar results of compression of the hyporheic zone, but in general report a net result of reducing the hyporheic residence time and increasing the hyporheic discharge with increasing heterogeneity of hydraulic conductivity (Sawyer and Cardenas, 2009; Gomez-Velez et al., 2014; Pryshlak et al., 2015; Laube et al., 2018).

Modeling of hyporheic exchange in gravel-bed rivers having a pool-riffle morphology (e.g., Montgomery and Buffington 1997) is more complex than dunes because the bedforms are three-dimensional and may be fully (Marzadri et al., 2010; Trauth et al., 2013) or partially (Tonina and Buffington, 2007; Monofy and Boano, 2021) submerged. For the fully-submerged case, semianalytical models show that the mean and variance of the residence time distribution (μ_t and σ_t, respectively) depend on streambed morphology and surface hydrology, such that (Marzadri et al., 2010)

$$\begin{aligned} \mu_t^* &= 1.39\, Y^{*0.6};\; R^2 = 0.96 \\ \mu_t &= \frac{\lambda \mu_t^*}{K_C s_i C_z} \end{aligned} \tag{3.9}$$

$$\begin{aligned} \sigma_t^{2*} &= 2.07\, Y^{*0.89};\; R^2 = 0.91 \\ \sigma_t^2 &= \left(\frac{\lambda}{K_C s_i C_z}\right)^2 \sigma_t^{2*} \end{aligned} \tag{3.10}$$

where μ^*_t and σ_t^{2*} are the dimensionless mean and variance of the residence time distribution, respectively, s_i is the streambed slope, and C_z is the dimensionless Chézy number

$$C_z = 6 + 2.5 \ln\left(\frac{1}{2.5\, d_s}\right) \tag{3.11}$$

with d_s ($=d_{50}/Y_0$) being the relative submergence of the sediment. The full hyporheic residence time can be approximated from the mean and variance, assuming a lognormal distribution (Marzadri et al., 2010; Tonina and Buffington, 2011). Similarly, the spatially averaged downwelling flow is estimated as (Tonina, 2012)

$$\begin{aligned} \overline{q}^* &= 41.108\, Y^{*-0.732};\; R^2 = 0.96 \\ \overline{q} &= \frac{\overline{q}^* K_C}{C_z^4} \end{aligned} \tag{3.12}$$

Semiempirical relationships, which account for the role of ambient groundwater (both basal (vertical) and underflow (horizontal)) are also available for fully submerged pool-riffle bedforms (Trauth et al., 2013).

For the case of partially submerged bars in gravel pool-riffle channels, the prediction of hyporheic exchange is based on empirical regressions (Tonina and Buffington, 2011; Trauth et al., 2013; Huang and Chui, 2018; Monofy and Boano, 2021), using a set of dimensional numbers such as those suggested by Tonina and Buffington (2011).

$$\Pi'_1 = \frac{\rho U Y_0}{\mu};\ \Pi'_2 = \frac{U}{\sqrt{g Y_0}};\ \Pi'_3 = \frac{\Delta}{Y_0};\ \Pi'_4 = \frac{\lambda}{Y_0};\ \Pi'_5 = s_i; \tag{3.13}$$

$$\prod\nolimits_1 = \frac{\rho U \sqrt{K}}{\mu};\ \prod\nolimits_2 = \frac{U^2}{g\sqrt{K}};\ \prod\nolimits_3 = \frac{Y_0}{\sqrt{K}};\ \prod\nolimits_4 = s_i;\ \prod\nolimits_5 = \frac{\Delta}{\lambda};\ \prod\nolimits_6 = \frac{d_b}{\sqrt{K}}; \tag{3.14}$$

where ρ is the fluid density, μ is the dynamic fluid viscosity, and K is the sediment permeability. The hyporheic exchange depth, d_h, and the mean, μ_t, and standard deviation, σ_t, of the hyporheic residence time distribution are then quantified as

$$\frac{d_h}{Y_0} = \exp\left(\sum_{i=1}^{5} A_i \ln\left(\Pi'_i\right)\right) \tag{3.15}$$

$$\frac{\mu_t U}{\sqrt{K}} = \exp\left(\sum_{i=1}^{6} B_i \ln\left(\prod\nolimits_i\right)\right) \tag{3.16}$$

$$\frac{\sigma_t U}{\sqrt{K}} = \exp\left(\sum_{i=1}^{6} B'_i \ln\left(\prod\nolimits_i\right)\right) \tag{3.17}$$

and the regression coefficients are reported in Table 3.1.

In contrast to dunes, pool-riffle sequences form at high flows near bankfull stage (e.g., Montgomery and Buffington, 1997, 1998), when gravel substrates are set in motion (Tubino, 1991). Thus, for applications with discharges lower than bankfull, the streambed morphology

TABLE 3.1 Empirically determined parameters for, Eqs. (3.15)–(3.17), respectively, as proposed by Tonina and Buffington (2011).

i		1	2	3	4	5	6
Mean hyporheic depth (3.15)	A_i	0.152	−0.058	−0.509	0.074	0.906	
Mean hyporheic residence time (3.16)	B_i	−0.682	0.387	1.619	0.314	−1.339	0.407
Standard deviation of the hyporheic residence time (3.17)	B'_i	−0.533	0.652	1.369	0.098	−1.066	0.456

in pool-riffle channels can be assumed stationary, while surface hydraulics change with discharge. Bedform length and amplitude can be predicted from bankfull width, W_b, and depth, Y_{0b}, such that: $\lambda = 6.5W_b$, and $\Delta = Y_{0b}/(0.18d_s^{0.45}\beta^{1.45})$, where β is the half-channel aspect ratio $\beta = Y_0/(2W)$ and valid for $2<\beta<35$ (Ikeda, 1984). Mean hydraulic width, W, depth, D, and velocity, U, can be estimated from discharge, Q, using hydraulic geometry relations: $W = 12.936Q^{0.423}$ ($R^2 = 0.82$), $D = 0.409Q^{0.294}$ ($R^2 = 0.62$) and $U = 0.196Q^{0.285}$ ($R^2 = 0.49$) (e.g., Raymond et al., 2012) for cases where only discharge is known as applied by Marzadri et al. (2017). In addition to the bar and pool topography of these channels, the protruding riffle volume above the mean streambed elevation may also induce hyporheic exchange. This mechanism is particularly important in low-gradient streams (Bray and Dunne, 2017), which typically have larger riffle amplitudes than steep streams (Marzadri et al., 2010).

The above investigations typically assume homogenous hydraulic conductivities, but gravel-bed rivers tend to have a complex stratigraphy (Dai et al., 2003; Ritzi et al., 2004) that produces chiefly categorical heterogeneity, which has been shown to have important implications for hyporheic exchange (Zhou et al., 2014; Pryshlak et al., 2015) in terms of reducing exchange depths and residence times, but increasing fluxes.

In addition to models developed for dune and pool-riffle channels, semiempirical solutions have been proposed for other in-channel features, such as channel-spanning logs (Sawyer et al., 2011), steps (Hester and Doyle, 2008), and fully-submerged semihemispherical features (e.g., boulders and cobbles) (Hutchinson and Webster, 1998). For sinuous channels, predictive models have been proposed for intrameandering flows (those due to pressure differences between meander bends) (Cardenas, 2009b; Boano et al., 2010a; Kiel and Cardenas, 2014), which typically have much longer residence times and flow paths than those induced by in-channel bedforms. However, predictive models are not yet available for reach-scale hyporheic flows induced by bedforms and cobble/boulder substrate in cascade, step-pool, and plane-bed streams (*sensu* Montgomery and Buffington, 1997), although the mechanics of hyporheic exchange in such channels are understood conceptually (Buffington and Tonina, 2009).

Reach and landscape scales

Reach-scale hyporheic models were originally developed to improve prediction of in-stream solute transport by accounting for transient storage zones, which are comprised of surface storage zones (e.g., backwaters, eddies, bank alcoves) and subsurface storage (the hyporheic zone), both of which are characterized by slower velocities than the mainstream flow, causing solutes to be retained and then released at later times. These surface and subsurface transient storage zones form concentration curves with long tails that traditional advection-dispersion-reaction equations, ADRE, do not model well. The One-dimensional Transport with Inflow and Storage (OTIS) program was the first to model this phenomenon (Runkel, 1998). OTIS models the surface transport with an ADRE that exchanges solute concentration with a fixed volume of transient storage using a first-order transfer function characterized by two parameters (storage area and exchange rate), plus two additional parameters for the stream water (cross-sectional area and an effective diffusion coefficient) (Runkel, 1998). The four parameters are typically calibrated with measured concentration breakthrough curves derived from surface tracer experiments (Harvey and Wagner, 2000) because of the lack of relationships between stream hydromorphological characteristics and storage zone parameters. Calibration is difficult because the problem suffers from equifinality, as there are four unknowns but only two equations (Mrokowska and Osuch, 2011). OTIS has been applied for simulating hyporheic exchange by assuming that most transient storage chiefly occurs in the hyporheic zone, with negligible storage in surface (in-channel) reservoirs (Bencala and Walters, 1983; Harvey et al., 1996; Harvey and Gorelick, 2000). This has been argued to be true in small steep streams (Mulholland et al., 1997), where most studies using OTIS have been conducted (Gooseff et al., 2006), as opposed to low-gradient channels that commonly have extensive surface storage zones (e.g., pools and backwaters), particularly in meandering floodplain rivers or forest channels with abundant wood debris (Montgomery and Buffington, 1997, 1998). Therefore, the transient storage approach is best applied to streams with few surface storage zones; models with multiple transient storage zones are available, but they are difficult to calibrate (Choi et al., 2000; Stewart et al., 2011). Transient storage models such as OTIS typically result in an exponential residence time distribution (transfer function between the surface flow and the hyporheic zone), which has been shown to poorly capture long exchange paths (i.e., the tail of the residence time distribution) (Zaramella et al., 2003). Nevertheless, transient storage models are a useful first-order approximation that captures the bulk of the hyporheic exchange because most of the exchange occurs in the shallow, near-surface portion of the hyporheic zone and is characterized by rapid exchange along short flow paths that are strongly coupled to surface hydraulics (Harvey and Wagner, 2000; Zaramella et al., 2003; Marzadri et al., 2010).

Other researchers have proposed different forms for the transfer function, which models the interaction between the stream water and the hyporheic zone. The transfer function is typically associated with hyporheic exchange driven by topographic features. For instance, Wörman et al. (2002) modeled the transfer function assuming pumping exchange driven by dune-like bedforms, which generates a lognormal residence time distribution. Other approaches, such as the Solute Transport and Multirate Mass Transfer-Linear Coordinates (STAMMT-L) model (Haggerty and Reeves, 2002) and the Solute Transport in Rivers (STIR) routine (Marion et al., 2008b) select different forms of the hyporheic residence time distribution. Boano et al. (2007a) adopted a continuous time random walk (CTRW) theory, which has been further developed into a double domain approach (one domain for the surface and one for the subsurface processes) (Sherman et al., 2019) for modeling surface and subsurface exchange. These methods have been successfully applied at both reach and valley-segment scales. Stonedahl et al. (2010) explored the role of different topographic scales (e.g., ripples, dunes, and planimetric features such as meanders) on hyporheic exchange as the domain increases from micro to channel-reach scales. They suggested a superposition of the effects of bedform-induced hyporheic exchange and showed the influence of local and large-scale topography on hyporheic exchange. They assumed that dynamic head variation dominates at the micro scale, which they modeled as dune-like bedforms, while piezometric head dominates at the channel-reach scale due to water-surface variations.

Numerical models of hyporheic exchange have typically been applied at channel-unit (individual bedforms) and channel-reach (sequences of bedforms) scales, but Wörman et al. (2006) proposed a generalized three-dimensional model that can be applied at landscape scales. Although, they assumed a sinusoidal streambed pressure distribution throughout the entire river network (which is only suited to dune-ripple channels) and an energy profile approximated by the land topography (rather than that of water-surface elevations), their study is an important attempt to model hyporheic exchange at broad scales using digital elevation models. More recently, Gomez-Velez and Harvey (2014) developed a quantitative landscape perspective of hyporheic exchange along river networks using the Networks with EXchange and Subsurface Storage (NEXSS) model. The approach employs available hyporheic models to quantify mean values of exchange at reach scales resulting from multiple topographic features. Marzadri et al. (2017) proposed a similar method, but their model focusses on the primary topographic feature in a given reach (e.g., dune or pool-riffle bedforms).

The role of hyporheic flow on water quality

Field observations (Triska et al., 1993; Argerich et al., 2011; Zarnetske et al., 2011) and large-scale flume experiments (Quick et al., 2016; Kaufman et al., 2017; De Falco et al., 2018) have quantified the role of hyporheic fluxes on reactive solutes and on water temperature as this regulates biogeochemical reactions. Hyporheic exchange affects both the chemical (Fig. 3.2) (Zarnetske et al., 2011) and temperature (Wu et al., 2020) regimes of pore water, as well as affecting surface-water characteristics (Triska et al., 1989b; Harvey et al., 2013). Similarly, numerical models that couple hydromorphological and biogeochemical processes using ADRE (Sheibley et al., 2003; Cardenas et al., 2008; Fanelli and Lautz, 2008; Marzadri et al., 2012; Zarnetske et al., 2012) support the importance of the hyporheic zone on reactive solute transformations for both surface and pore waters (Fig. 3.3). These numerical models, which typically solve the groundwater flow based on homogenous hydraulic conductivity and Darcy's flow velocity, are chiefly run at the bedform (Cardenas et al., 2008; Trauth et al., 2013) or stream reach (Fleckenstein et al., 2006; Lautz and Siegel, 2006) scales, where sufficient information about boundary conditions (e.g., streambed topography, discharge, and water stage) are available (e.g., Fig. 3.3A). Results typically include detailed mapping of the hyporheic flow field (magnitude and direction of flow, Fig. 3.3B) and hyporheic residence time (Fig. 3.3C), which have important implications for water quality and locations of upwelling and downwelling fluxes at the streambed surface. Adoption of a Lagrangian reference system, where transport is modeled along flowlines (assuming negligible transversal exchange), simplifies the problem from three dimensional to one dimensional, replacing the horizontal (x, y) and vertical (z) Cartesian coordinates with travel time, τ, which is the time that a particle spends traversing the hyporheic zone along a given flowline between downwelling into the subsurface and upwelling back into the stream. This Lagrangian approach allows the prediction of hyporheic water quality, including temperature (Fig. 3.3D) and reactive solute concentrations (Fig. 3.3E) along flowlines based on τ only. Numerical modeling supported by accurate boundary conditions has been shown to provide good predictions of hyporheic processes, including mapping of hyporheic velocity and concentrations of reaction solutes (e.g., Janssen et al., 2012; Cardenas et al., 2016; Reeder et al., 2019; Trauth et al., 2014), although such approaches are limited to small well-characterized domains and well-constrained field applications (Marzadri et al., 2013a; Tonina et al., 2015).

Heterogeneity of streambed sediment can further strengthen the hyporheic zone as a hot spot for biogeochemical transformations, as recent numerical simulations have shown that mixtures of sands and silts have a high capacity to remove nitrate (Pescimoro et al., 2019).

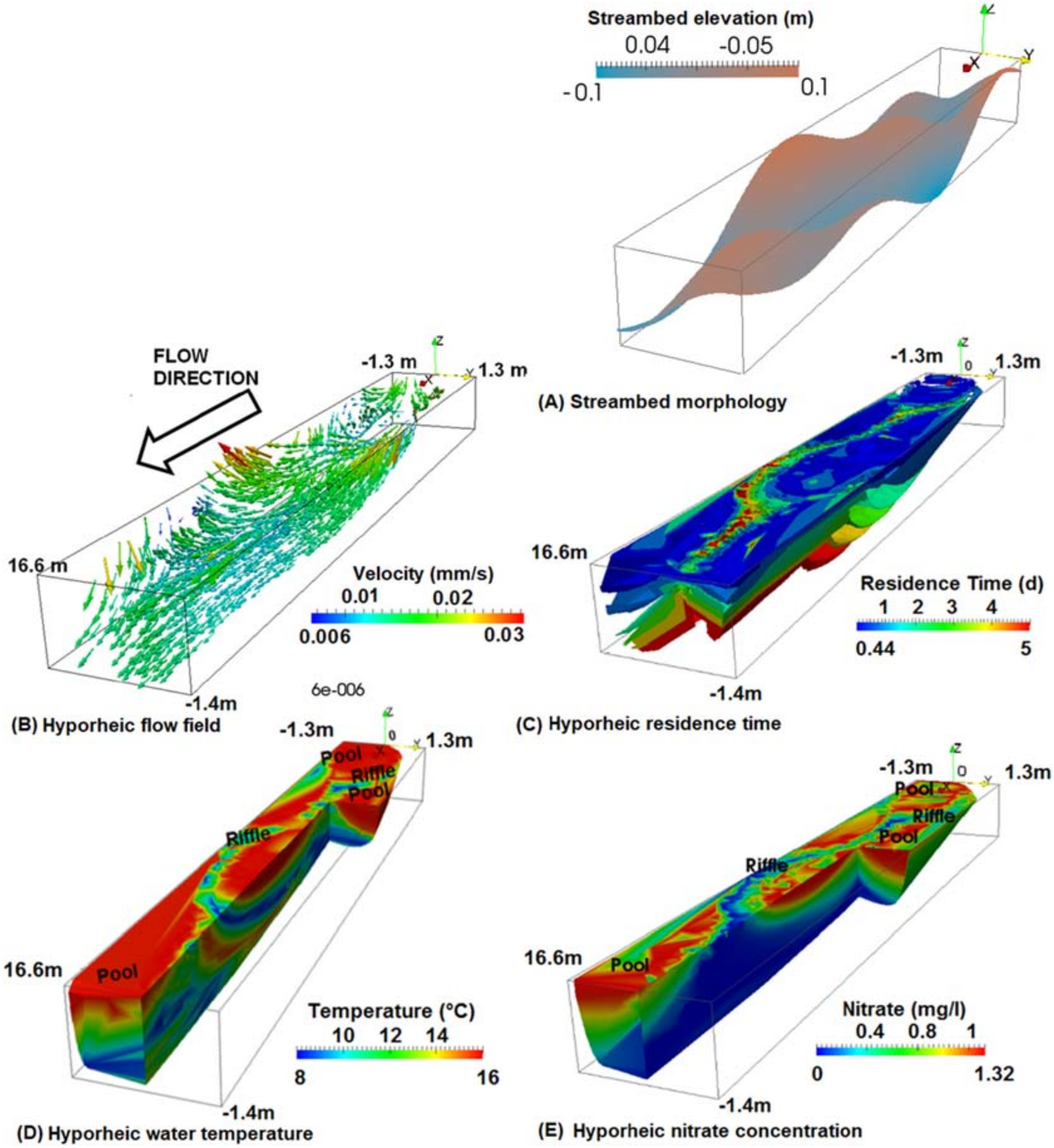

FIGURE 3.3 Pool-riffle morphology (A) induced hyporheic flow field (magnitude and direction of flow velocity) (B), residence time (shown as isotemporal curves) (C), water temperature (D), and nitrate concentration (E) simulated with a Lagrangian advection dispersion and reaction (ADRE) model presented by Marzadri et al. (2010, 2011, 2012, 2013a, 2013b). Hyporheic exchange was induced by a fully-submerged pool-riffle morphology (A), with bedform length of 17 m and amplitude of 0.2 m, for a mean streamflow depth of 0.1 m, discharge of 0.18 m^3/s, and a sediment thickness of 2.6 m. In-stream concentrations of dissolved oxygen were at saturation and that of nitrates at 1.32 mg/L, while stream water temperature changed sinusoidally through the day, with an amplitude of 8°C and a mean temperature of 12°C. Input parameters and model description are further detailed in Marzadri et al. (2010, 2011, 2012, 2013a, 2013b)

This mechanism could be used to enhance stream nutrient removal in systems where nutrients are problematic (Herzog et al., 2016). Furthermore, the spatial distribution of reaction rate constants may structure biological heterogeneity and the subsequent occurrence of biogeochemical hotspots within the hyporheic zone (Reeder et al., 2018a). However, the importance of the hyporheic zone on surface water quality is expected to be stream-size dependent (Wondzell, 2011), with hyporheic processes dominating biogeochemical reactions in small streams (Naegeli and Uehlinger, 1997; Marzadri et al., 2017) (channel widths, W, less than 10 m), but having a lesser effect in intermediate ($10\ \mathrm{m} < W < 100\ \mathrm{m}$) streams, and a negligible influence in larger rivers ($W > 100\ \mathrm{m}$) (Marzadri et al., 2022). For instance, recent studies on nitrous oxide emissions from streams and rivers show that the hyporheic zone is the main source of N_2O in small streams, whereas the *benthic zone* (stream bottom and shallow subsurface sediment reached by sunlight) becomes important for larger streams (Marzadri et al., 2017, 2022). For large rivers ($W > 100\ \mathrm{m}$), such as the upper Mississippi, biogeochemical reactions within the water column are the main source of N_2O (Marzadri et al., 2020). Four physical causes have been suggested for the reduced importance of the hyporheic zone relative to instream processes in controlling biogeochemical reactions with increasing river size: (1) lower rates of exchange between surface and subsurface flows due to systematic decreases in hydraulic conductivity as one moves downslope from small streams with gravel beds (high permeability) to large rivers with sand and gravel mixtures or sand and silt substrates (low permeability); (2) the above reduction in exchange combined with systematic increases in surface discharge as watercourses become larger causes a smaller ratio of hyporheic-to-instream discharge (Wondzell, 2011), (3) lower reaction-rate constants within streambed sediments, potentially due to low interstitial velocities (Reeder et al., 2018b), and (4) increases in the density and diversity of microbial communities and biofilms in the water column (Liu et al., 2013; Reisinger et al., 2015) due to increases in suspended sediment, which provide the supportive matrix for these organisms (Xia et al., 2009).

Numerical models at bedform and reach scales have highlighted the role of stream topography, stream flow, groundwater flow, and hyporheic fluxes in controlling biogeochemical reactions (Fig. 3.3). However, application of these models at river-network scales is unfeasible. Recent studies, rooted in the Lagrangian approach (Ocampo et al., 2006; Marzadri et al., 2012; Zarnetske et al., 2012; Hampton et al., 2020), suggest that biogeochemical processes may scale with the Damköhler number, Da, defined as the ratio between the characteristic time scales of fluid advection and biogeochemical transformation. At the scale of individual flowlines, the advective time is simply the travel time, τ, of the fluid along the flowline (Marzadri et al., 2012). However, at bedform scales, hyporheic flow has a distribution of residence times, which can be indexed by the median value, τ_{50}, to describe overall response to the bedform. Thus, at bedform and reach scales, Da is defined as the ratio between the corresponding τ_{50} and the time scale of a given biogeochemical process, τ_{lim}, expressed as the inverse of the reaction rate constant, K_{re}

$$Da = \frac{\tau_{50}}{\tau_{lim}} = \tau_{50}\, K_{re} \tag{3.18}$$

This approach has been shown to be effective for nitrous oxide, N_2O, emissions in streams, with potential extension to other biogeochemical reactions (Zarnetske et al., 2011; Marzadri et

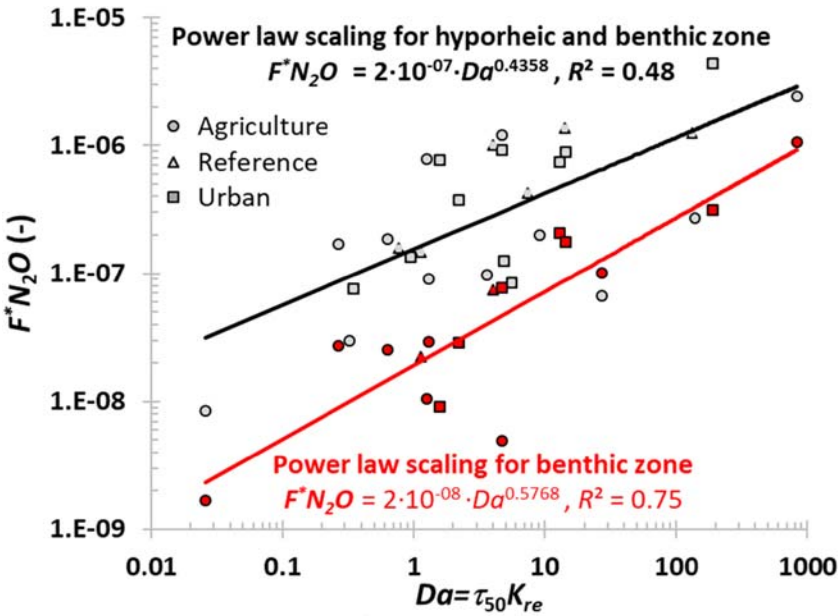

FIGURE 3.4 Reach-scale dimensionless N_2O fluxes, F^*N_2O, generated from the benthic (red) and combined benthic—hyporheic (gray) zones of headwater streams (channel widths less than 10 m) with pool-riffle or dune morphologies as a function of Damköhler number, Da, where τ_{50} is the median residence time of the hyporheic flow and K_{re} is the reaction rate constant of denitrification, defined as the uptake rate normalized by the mean flow depth of the channel. F^*N_2O is defined as the N_2O flux per unit area scaled by the total in-stream flux of a given dissolved inorganic nitrogen species (NO_3^- and NH_4^+). Data are from the Kalamazoo River (Michigan) (Beaulieu et al., 2008, 2009) and the second Lotic Intersite Nitrogen eXperiment (LINXII), which includes sites throughout the United States and Puerto Rico, spanning a broad range of land use, land cover, biomes, climatic zones, and channel morphologies (Mulholland et al., 2008). Following Mulholland et al.'s (2008) classification, reference streams had more than 85% native vegetation, while agricultural and urban streams drained watersheds with varying proportions of those land-cover types, respectively. *Modified from Marzadri et al. (2017).*

al., 2012, 2022). In particular, analysis of data from headwater streams shows that the reach-scale dimensionless flux of N_2O, F^*N_2O, exhibits a power-law scaling with Da that is independent of land use, ecohydromorphology, or climate (Marzadri et al., 2017) (Fig. 3.4). The study showed that the production of N_2O from the benthic layer (red curve in Fig. 3.4) was almost an order of magnitude smaller than that from the combined emissions of the benthic and hyporheic zones in these small streams (black curve in Fig. 3.4). The two empirical power laws were then applied to a set of more than 400 stream reaches worldwide, providing good predictive power (Marzadri et al., 2017).

The above analyses also show that not only are reactant loads (or concentrations) important, but stream morphology and hydraulics can regulate the amount of products generated (Marzadri et al., 2014). This is probably due to the fact that hyporheic exchange depends on stream hydromorphology (e.g., Buffington and Tonina 2009), which, in turn, may specialize the distribution of microbial communities and functioning (Quick et al., 2016). For example, microbes having the nirS gene, associated with denitrifying enzymes, cluster at the interface between the aerobic—anaerobic zone, the position of which is controlled by both flow hydraulics and biogeochemical reaction rates (cf. Fig. 3.2G and H). Overall, local-scale processes within the hyporheic zone, benthic zone, and surface water column may have important effects at the global scale, because they may regulate riverine production of N_2O and, thus, should be accounted for in predicting the impact of anthropogenic activities on biogeochemical processes in riverine systems (e.g., Marzadri et al., 2021).

Conclusion

Surface water of alluvial rivers ubiquitously flows into and out of the interstitial spaces of the surrounding alluvium, creating a highly connected riverine ecosystem that extends well beyond the visible surface flow of rivers (Poole et al., 2008; Hauer et al., 2016). The extent of these flows depends on local conditions across multiple scales, including bed-surface grain size and heterogeneity, presence of microroughness elements (e.g., logs, boulders, biotic mounds), morphological characteristics of the stream (e.g., meso-scale variation of bed topography, flow depth, width, velocity), reach- to valley-scale morphology (macro-scale variation of bedform sequences, slope, confinement, and alluvial volume), associated geologic constraints, and the position of the groundwater table (Krause et al., 2022). These different scales of physical conditions and constraints form a hierarchy of nested hyporheic cells, with larger scales enveloping smaller ones (Baxter and Hauer, 2000; Malard et al., 2002; Poole et al., 2008; Buffington and Tonina, 2009; Stonedahl et al., 2013). As the size of hyporheic cells increases, so does the residence time of stream water traversing the hyporheic zone, while the average interstitial flow velocity is reduced because pressure gradients become smaller over longer distances between two points. The net result is a set of nested transient storage zones, where biogeochemical reactions transform reactive solutes, with resultant products upwelling into the surface streamflow. These physical and chemical gradients have important implications for water quality in both surface and pore waters. However, the importance of hyporheic exchange on surface water quality is expected to be stream-size dependent, because as stream size increases, the ratio between hyporheic discharge and surface discharge decreases (Wondzell, 2011), diluting hyporheic products within the surface water.

The fading of the importance of hyporheic processes on surface water quality in larger rivers is still under investigation, but the hyporheic zone is expected to remain an important and key element of river corridors even in large rivers as it may provide localized thermal, chemical, and hydraulic refugia for aquatic species, particularly in upwelling zones (Baxter and Hauer, 2000; Malard et al., 2002; Stanford et al., 2005; see review by Wondzell, 2011). In addition, the hyporheic zone has become a key element in stream and river restoration (Hester and Gooseff, 2010; Ward et al., 2011; Herzog et al., 2016), particularly where engineering solutions are required to better design this environment. Overall, a broad range of investigations are exploring the impact of morphological and biological heterogeneities on hyporheic conditions and how hyporheic processes respond to dynamic changes of solutes (Marzadri et al., 2013b; Kaufman et al., 2017) and surface and groundwater hydraulics (Krause et al., 2022). Furthermore, local hyporheic processes are being upscaled to more broadly predict water quality within riverine systems at watershed and regional scales (e.g., to address nutrient removal and greenhouse gas emissions) (Stewart et al. 2011; Gomez-Velez and Harvey, 2014; Marzadri et al., 2017, 2021). These investigations may be supported by novel methodologies (1) in the laboratory, e.g., non-invasive approaches like optical measurements (Cardenas et al., 2016; Reeder et al., 2018b) and image analysis coupled with refractive index matching, RIM, which allows mapping of the flow field through solid grains (Voermans et al., 2018; Moreto et al., 2022) with biological activities (Rubol et al., 2018) and (2) in the field, including optical measurements (Vieweg et al., 2013; Reeder et al., 2019) and improved data analysis (e.g., water temperature time series (van Kampen et al., 2022)) and (3) data assimilation and distribution via machine learning (Marzadri et al., 2021) and numerical simulations (Chowdhury et al., 2020; Shen et al., 2020; Yuan et al., 2021).

Acknowledgments

We thank Annika Quick, William Jeff Reeder and Alessandra Marzadri for providing data and helping with Figs. 3.2−3.4. Data were collected and analyzed with support from NSF grants 1141690, 1141752, 1344661, 1344602 and IIA-1301792 D.T. acknowledges support from the USDA National Institute of Food and Agriculture, Hatch project 1012806. We thank F. Boano for constructive comments that improved this chapter.

References

Alley, W.M., Reilly, T.E., Franke, O.L., 1999. Sustainability of Ground-Water Resources. US Geological Survey, Circular 1186, Denver, CO.

Argerich, A., Haggerty, R., Martí, E., Sabater, F., Zarnetske, J., 2011. Quantification of metabolically active transient storage (MATS) in two reaches with contrasting transient storage and ecosystem respiration. Journal of Geophysical Research: Biogeosciences 116, G03034.

Baxter, C.V., Hauer, F.R., 2000. Geomorphology, hyporheic exchange, and selection of spawning habitat by bull trout (*Salvelinus confluentus*). Canadian Journal of Fisheries and Aquatic Sciences 57 (7), 1470−1481. https://doi.org/10.1139/f00-056.

Beaulieu, J.J., Arango, C.P., Hamilton, S.K., Tank, J.L., 2008. The production and emission of nitrous oxide from headwater streams in the Midwestern United States. Global Change Biology 14 (4), 878−894. https://doi.org/10.1111/j.1365-2486.2007.01485.x.

Beaulieu, J.J., Arango, C.P., Tank, J.L., 2009. The effects of season and agriculture on nitrous oxide production in headwater streams. Journal of Environment Quality 38 (2), 637−646. https://doi.org/10.2134/jeq2008.0003.

Bencala, K.E., Walters, R.A., 1983. Simulation of solute transport in a mountain pool-and-riffle stream: a transient storage model. Water Resources Research 19 (3), 718−724.

Blois, G., Best, J.L., Sambrook Smith, G.H., Hardy, R.J., 2014. Effect of bed permeability and hyporheic flow on turbulent flow over bed forms. Geophysical Research Letters 41 (18), 6435−6442.

Boano, F., Camporeale, C., Revelli, R., 2010a. A linear model for the coupled surface-subsurface flow in a meandering stream. Water Resources Research 46, W07535.

Boano, F., Camporeale, C., Revelli, R., Ridolfi, L., 2006. Sinuosity-driven hyporheic exchange in meandering rivers. Geophysical Research Letters 33, L18406. https://doi.org/10.1029/2006GL027630.

Boano, F., Harvey, J.W., Marion, A., Packman, A.I., Revelli, R., Ridolfi, L., Wörman, A., 2014. Hyporheic flow and transport processes: mechanisms, models, and biogeochemical implications. Reviews of Geophysics 52 (4), 603−679. https://doi.org/10.1002/2012RG000417.

Boano, F., Packman, A.I., Cortis, A., Revelli, R., Ridolfi, L., 2007a. A continuous time random walk approach to the stream transport of solutes. Water Resources Research 43, W10425.

Boano, F., Poggi, D., Revelli, R., Ridolfi, L., 2009. Gravity-driven water exchange between streams and hyporheic zones. Geophysical Research Letters 36, L20402.

Boano, F., Revelli, R., Ridolfi, L., 2007b. Bedform-induced hyporheic exchange with unsteady flows. Advances in Water Resources 30, 148−156.

Boano, F., Revelli, R., Ridolfi, L., 2008. Reduction of the hyporheic zone volume due to the stream-aquifer interaction. Geophysical Research Letters 35, L09401.

Boano, F., Revelli, R., Ridolfi, L., 2010b. Effect of streamflow stochasticity on bedform-driven hyporheic exchange. Advances in Water Resources 33, 1367–1374.

Boano, F., Revelli, R., Ridolfi, L., 2013. Modeling hyporheic exchange with unsteady stream discharge and bedform dynamics. Water Resources Research 49, 4089–4099. https://doi.org/10.1002/wrcr.20322.

Bott, T.L., Kaplan, L.A., Kuserk, F.T., 1984. Benthic bacterial biomass supported by stream water dissolved organic matter. Microbial Ecology 10, 335–344.

Bottacin-Busolin, A., Marion, A., 2010. Combined role of advective pumping and mechanical dispersion on time scales of bed form–induced hyporheic exchange. Water Resources Research 46, W08518. https://doi.org/10.1029/2009WR008892.

Bray, E.N., Dunne, T., 2017. Subsurface flow in lowland river gravel bars. Water Resources Research 53 (9), 7773–7797.

Briggs, M.A., Lautz, L.K., Hare, D.K., González-Pinzón, R., 2013. Relating hyporheic fluxes, residence times, and redox-sensitive biogeochemical processes upstream of beaver dams. Freshwater Science 32 (2), 622–641. https://doi.org/10.1899/12-110.1.

Briggs, M.A., Lautz, L.K., McKenzie, J.M., Gordon, R.P., Hare, D.K., 2012. Using high-resolution distributed temperature sensing to quantify spatial and temporal variability in vertical hyporheic flux. Water Resources Research 48, W02527.

Buffington, J.M., Tonina, D., 2009. Hyporheic exchange in mountain rivers II: effects of channel morphology on mechanics, scales, and rates of exchange. Geography Compass 3 (3), 1038–1062. https://doi.org/10.1111/j.1749-8198.2009.00225.x.

Cardenas, M.B., 2007. Potential contribution of topography-driven regional groundwater flow to fractal stream chemistry: residence time distribution analysis of Tóth flow. Geophysical Research Letters 34, L05403.

Cardenas, M.B., 2009a. Stream-aquifer interactions and hyporheic exchange in gaining and losing sinuous streams. Water Resources Research 45, W06429.

Cardenas, M.B., 2009b. A model for lateral hyporheic flow based on valley slope and channel sinuosity. Water Resources Research 45 (1), W01501. https://doi.org/10.1029/2008WR007442.

Cardenas, M.B., Wilson, J.L., 2007a. Dunes, turbulent eddies, and interfacial exchange with permeable sediments. Water Resources Research 43, W08412.

Cardenas, M.B., Wilson, J.L., 2007b. Exchange across a sediment–water interface with ambient groundwater discharge. Journal of Hydrology 346, 69–80.

Cardenas, M.B., Zlotnik, V.A., 2003. Three-dimensional model of modern channel bend deposits. Water Resources Research 39 (6), 1141. https://doi.org/10.1029/2002WR001383.

Cardenas, M.B., Cook, P.L.M., Jiang, H., Traykovski, P., 2008. Constraining denitrification in permeable wave-influenced marine sediment using linked hydrodynamic and biogeochemical modeling. Earth and Planetary Science Letters 275 (1–2), 127–137.

Cardenas, M.B., Ford, A.E., Kaufman, M.H., Kessler, A.J., Cook, P.L.M., 2016. Hyporheic flow and dissolved oxygen distribution in fish nests: the effects of open channel velocity, permeability patterns, and groundwater upwelling. Journal of Geophysical Research: Biogeosciences 121, 3113–3130.

Castro, N.M., Hornberger, G.M., 1991. Surface-subsurface water interaction in an alluviated mountain stream channel. Water Resources Research 27 (7), 1613–1621.

Chen, X., Cardenas, M.B., Chen, L., 2015. Three-dimensional versus two-dimensional bed form-induced hyporheic exchange. Water Resources Research 51, 2923–2936. https://doi.org/10.1002/2014WR016848.

Chen, X., Cardenas, M.B., Chen, L., 2018. Hyporheic exchange driven by three-dimensional sandy bed forms: sensitivity to and prediction from bed form geometry. Water Resources Research 54 (6), 4131–4149. https://doi.org/10.1029/2018WR022663.

Choi, J., Harvey, J.W., Conklin, M.H., 2000. Characterizing multiple timescales of stream and storage zone interaction that affect solute fate and transport in streams. Water Resources Research 36 (6), 1511–1518.

Chowdhury, R.S., Zarnetske, J.P., Phanikumar, M.S., Briggs, M.A., Day-Lewis, F.D., Singha, K., 2020. Formation criteria for hyporheic anoxic microzones: assessing interactions of hydraulics, nutrients, and biofilms. Water Resources Research 56 (3), e2019WR025971. https://doi.org/10.1029/2019WR025971.

Constantz, J., 2008. Heat as a tracer to determine streambed water exchanges. Water Resources Research 44, W00D10.

Cooper, A.C., 1965. The effect of transported stream sediments on the survival of sockeye and pink salmon eggs and alevin. International Pacific Salmon Fisheries Commission Bulletin 18, New Westminster, BC, Canada.

Cranswick, R.H., Cook, P.G., Lamontagne, S., 2014. Hyporheic zone exchange fluxes and residence times inferred from riverbed temperature and radon data. Journal of Hydrology 519, 1870−1881. https://doi.org/10.1016/j.jhydrol.2014.09.059.

Dai, Z., Ritzi, R.W., Dominic, D.F., Rubin, Y.N., 2003. Estimating spatial correlation structure for permeability in sediments with hierarchical organization. In: Mishra, S. (Ed.), Probabilistic Approaches to Groundwater Modeling Symposium 2003. American Society of Civil Engineers, New York, NY.

Dent, C.L., Grimm, N.B., Fisher, S.G., 2001. Multiscale effects of surface-subsurface exchange on stream water nutrient concentrations. Journal of the North American Benthological Society 20 (2), 162−181.

Drummond, J.D., Aubeneau, A., Packman, A.I., 2014. Stochastic modeling of fine particulate organic carbon dynamics in rivers. Water Resources Research 50 (5), 4341−4356.

Dudunake, T., Tonina, D., Reeder, W.J., Monsalve, A., 2020. Local and reach-scale hyporheic flow response from boulder-induced geomorphic changes. Water Resources Research 56 (10). https://doi.org/10.1029/2020WR027719.

Edwards, R.T., 1998. The hyporheic zone. In: Naiman, R.J., Bilby, R.E. (Eds.), River Ecology and Management: Lessons From the Pacific Coastal Ecoregion. Springer-Verlag, New York, NY, pp. 399−429.

Elliott, A.H., 1990. Transfer of Solutes Into and Out of Streambeds, Rep. KH-R-52. W.M. Keck Laboratory of Hydraulics and Water Resources, California Institute of Technology, Pasadena, CA.

Elliott, A.H., Brooks, N.H., 1997. Transfer of nonsorbing solutes to a streambed with bed forms: laboratory experiments. Water Resources Research 33 (1), 137−151.

De Falco, N., Boano, F., Bogler, A., Bar-Zeev, E., Arnon, S., 2018. Influence of stream-subsurface exchange flux and bacterial biofilms on oxygen consumption under nutrient-rich conditions. Journal of Geophysical Research: Biogeosciences 123 (7), 2021−2034.

Fanelli, R.M., Lautz, L.K., 2008. Patterns of water, heat and solute flux through streambeds around small dams. Ground Water 46 (5), 671−687.

Findlay, S., Strayer, W., Goumbala, C., Gould, K., 1993. Metabolism of streamwater dissolved organic carbon in the shallow hyporheic zone. Limnology & Oceanography 38, 1493−1499.

Fleckenstein, J.H., Niswonger, R.G., Fogg, G.E., 2006. River-aquifer interactions, geologic heterogeneity, and low-flow management. Ground Water 44, 837−852.

Fox, A., Boano, F., Arnon, S., 2014. Impact of losing and gaining streamflow conditions on hyporheic exchange fluxes induced by dune-shaped bed forms. Water Resources Research 50, 1895−1907.

Gariglio, F.P., Tonina, D., Luce, C.H., 2013. Spatio-temporal variability of hyporheic exchange through a pool-riffle-pool sequence. Water Resources Research 49 (11), 7185−7204. https://doi.org/10.1002/wrcr.20419.

Gibert, J., Stanford, J.A., Dole-Olivier, M.-J., Ward, J.V., 1994. Basic attributes of groundwater ecosystems and prospects for research. In: Gilbert, J., Danielpol, D.L., Standford, J.A. (Eds.), Groundwater Ecology. Academic Press, San Diego, CA, pp. 8−40.

Gomez-Velez, J.D., Harvey, J.W., 2014. A hydrogeomorphic river network model predicts where and why hyporheic exchange is important in large basins. Geophysical Research Letters 41 (18), 6403−6412. https://doi.org/10.1002/2014GL061099.

Gomez-Velez, J.D., Harvey, J.W., Cardenas, M.B., Kiel, B., 2015. Denitrification in the Mississippi River network controlled by flow through river bedforms. Nature Geoscience 8 (October), 1−8. https://doi.org/10.1038/ngeo2567.

Gomez-Velez, J.D., Krause, S., Wilson, J.L., 2014. Effect of low-permeability layers on spatial patterns of hyporheic exchange and groundwater upwelling. Water Resources Research 50, 5196−5215.

González-Pinzón, R., Haggerty, R., Myrold, D.D., 2012. Measuring aerobic respiration in stream ecosystems using the resazurin-resorufin system. Journal of Geophysical Research 117, G00N06.

Gooseff, M.N., 2010. Defining hyporheic zones- Advancing our conceptual and operational definitions of where stream water and groundwater meet. Geography Compass 4 (8), 945−955.

Gooseff, M.N., McGlynn, B.L., 2005. A stream tracer technique employing ionic tracers and specific conductance data applied to the Maimai catchment, New Zealand. Hydrological Processes 19, 2491−2506. https://doi.org/10.1002/hyp.5685.

Gooseff, M.N., Anderson, J.K., Wondzell, S.M., LaNier, J., Haggerty, R., 2006. A modelling study of hyporheic exchange pattern and the sequence, size, and spacing of stream bedforms in mountain stream networks, Oregon, USA. Hydrological Processes 20 (11), 2443–2457.

Gooseff, M.N., Hall, R.O.J., Tank, J.L., 2007. Relating transient storage to channel complexity in streams of varying land use in Jackson Hole, Wyoming. Water Resources Research 43, W01417.

Grant, S.B., Gomez-Velez, J.D., Ghisalberti, M., 2018. Modeling the effects of turbulence on hyporheic exchange and local-to-global nutrient processing in streams. Water Resources Research 54 (9), 5883–5889. https://doi.org/10.1029/2018WR023078.

Grant, S.B., Monofy, A., Boano, F., Gomez-Velez, J.D., Guymer, I., Harvey, J., Ghisalberti, M., 2020. Unifying advective and diffusive descriptions of bedform pumping in the benthic biolayer of streams. Water Resources Research 56 (11), e2020WR027967. https://doi.org/10.1029/2020WR027967.

Haggerty, R., Wondzell, S.M., Johnson, M.A., 2002. Power-law residence time distribution in hyporheic zone of a 2nd-order mountain stream. Geophysical Research Letters 29 (13), 4.

Haggerty, R., Reeves, P., 2002. STAMM-L Version 1.0 User's Manual. Sandia National Laboratory, Albuquerque, NM.

Haggerty, R., Martí, E., Argerich, A., von Schiller, D., Grimm, N.B., 2009. Resazurin as a "smart" tracer for quantifying metabolically active transient storage in stream ecosystems. Journal of Geophysical Research 114 (G3), G03014. https://doi.org/10.1029/2008JG000942.

Harvey, A.M., Wagner, B.J., 2000. Quantifying hydrologic interactions between streams and their subsurface hyporheic zones. In: Jones, J.B., Mulholland, P.J. (Eds.), Streams and Ground Waters. Academic Press, San Diego, CA, pp. 3–44.

Hampton, T.B., Zarnetske, J.P., Briggs, M.A., MahmoodPoor Dehkordy, F., Singha, K., Day-Lewis, F.D., Harvey, J.W., Chowdhury, S.R., Lane, J.W., 2020. Experimental shifts of hydrologic residence time in a sandy urban stream sediment–water interface alter nitrate removal and nitrous oxide fluxes. Biogeochemistry 149 (2), 195–219. https://doi.org/10.1007/s10533-020-00674-7.

Harvey, C., Gorelick, S.M., 2000. Rate-limited mass transfer or macrodispersion: which dominates plume evolution at the Macrodispersion Experiment (MADE) site? Water Resources Research 36 (3), 637–650.

Harvey, J.W., Bencala, K.E., 1993. The effect of streambed topography on surface-subsurface water exchange in mountain catchments. Water Resources Research 29 (1), 89–98. https://doi.org/10.1029/92WR01960.

Harvey, J.W., Böhlke, J.K., Voytek, A.M., Scott, D., Tobias, C.R., 2013. Hyporheic zone denitrification: controls on effective reaction depth and contribution to whole-stream mass balance. Water Resources Research 49 (10), 6298–6316.

Harvey, J.W., Drummond, J.D., Martin, R.L., McPhillips, L.E., Packman, A.I., Jerolmack, D.J., Stonedahl, S.H., Aubeneau, A.F., Sawyer, A.H., Larsen, L.G., Tobias, C.R., 2012. Hydrogeomorphology of the hyporheic zone: stream solute and fine particle interactions with a dynamic streambed. Journal of Geophysical Research: Biogeosciences 117, G00N11.

Harvey, J.W., Wagner, B.J., Bencala, K.E., 1996. Evaluating the reliability of the stream tracer approach to characterize stream-subsurface water exchange. Water Resources Research 32 (8), 2441–2451.

Hassan, M.A., Tonina, D., Beckie, R.D., Kinnear, M., 2015. The effects of discharge and slope on hyporheic flow in step-pool morphologies. Hydrological Processes 29 (3), 419–433. https://doi.org/10.1002/hyp.10155.

Hatch, C., Fisher, A.T., Revenaugh, J.S., Constantz, J., Ruehl, C., 2006. Quantifying surface water–groundwater interactions using time series analysis of streambed thermal records: method development. Water Resources Research 42, W10410.

Hauer, F.R., Locke, H., Dreitz, V.J., Hebblewhite, M., Lowe, W., Muhfeld, C., Nelson, C., Proctor, M., Rood, S., 2016. Gravel-bed river floodplains are the ecological nexus of glaciated mountain landscapes. Science Advances 2 (6), 2:e1600026. https://doi.org/10.1126/sciadv.1600026.

Herzog, S.P., Higgins, C.P., McCray, J.E., 2016. Engineered streambeds for induced hyporheic flow: enhanced removal of nutrients, pathogens, and metals from urban streams. Journal of Environmental Engineering 142 (1), 1–10. https://doi.org/10.1061/(ASCE)EE.1943-7870.0001012.

Hester, E.T., Cardenas, M.B., Haggerty, R., Apte, S.V., 2017. The importance and challenge of hyporheic mixing. Water Resources Research 53 (5), 3565–3575.

Hester, E.T., Doyle, M.W., 2008. In-stream geomorphic structures as drivers of hyporheic exchange. Water Resources Research 44 (3), W03417. https://doi.org/10.1029/2006WR005810.

Hester, E.T., Gooseff, M.N., 2010. Moving beyond the banks: hyporheic restoration is fundamental to restoring ecological services and functions of streams. Environmental Science and Technology 44 (5), 1521−1525. https://doi.org/10.1021/es902988n.

Hester, E.T., Young, K.I., Widdowson, M.A., 2013. Mixing of surface and groundwater induced by riverbed dunes: implications for hyporheic zone definitions and pollutant reactions. Water Resources Research 49, 5221−5237.

Huang, P., Chui, T.F.M., 2018. Empirical equations to predict the characteristics of hyporheic exchange in a pool-riffle sequence. Ground Water 56 (6), 947−958. https://doi.org/10.1111/gwat.12641.

Hutchinson, P.A., Webster, I.T., 1998. Solute uptake in aquatic sediment due to current-obstacle interactions. Journal of Environmental Engineering 124 (5), 419−426. https://doi.org/10.1061/(ASCE)0733-9372(1998)124:5(419).

Ikeda, S., 1984. Prediction of alternate bar wavelength and height. Journal of Hydraulic Engineering 110, 371−386.

Janssen, F., Cardenas, M.B., Sawyer, A.H., Dammrich, T., Krietsch, J., Beer, D., 2012. A comparative experimental and multiphysics computational fluid dynamics study of coupled surface−subsurface flow in bed forms. Water Resources Research 48 (8), W08514.

Janssen, F., Huettel, M., Witte, U., Faerber, P., Huettel, M., Meyer, V., Witte, U., 2005. Pore-water advection and solute fluxes in permeable marine sediments (I): calibration and performance of the novel benthic chamber system Sandy. Limnology & Oceanography 50 (3), 768−778. https://doi.org/10.4319/lo.2005.50.3.0779.

Kaufman, M.H., Cardenas, M.B., Buttles, J., Kessler, A.J., Cook, P.L.M., 2017. Hyporheic hot moments: dissolved oxygen dynamics in the hyporheic zone in response to surface flow perturbations. Water Resources Research 53, 6642−6662.

Kiel, B.A., Cardenas, M.B., 2014. Lateral hyporheic exchange throughout the Mississippi River network. Nature Geoscience 7 (6), 413−417. https://doi.org/10.1038/ngeo2157.

Knapp, J.L.A., González-Pinzón, R., Drummond, J.D., Larsen, L.G., Cirpka, O.A., Harvey, J.W., 2017. Tracer-based characterization of hyporheic exchange and benthic biolayers in streams. Water Resources Research 53 (2), 1575−1594. https://doi.org/10.1002/2016WR019393.

Krause, S., Abbott, B.W., Baranov, V., Bernal, S., Blaen, P., Datry, T., Drummond, J., Fleckenstein, J.H., Velez, J.G., Hannah, D.M., Knapp, J.L.A., Kurz, M., Lewandowski, J., Martí, E., Mendoza-Lera, C., Milner, A., Packman, A., Pinay, G., Ward, A.S., Zarnetzke, J.P., 2022. Organizational principles of hyporheic exchange flow and biogeochemical cycling in river networks across scales. Water Resources Research 58 (3), e2021WR029771. https://doi.org/10.1029/2021WR029771.

Laube, G., Schmidt, C., Fleckenstein, J.H., 2018. The systematic effect of streambed conductivity heterogeneity on hyporheic flux and residence time. Advances in Water Resources 122, 60−69. https://doi.org/10.1016/j.advwatres.2018.10.003.

Lautz, L.K., Siegel, D.I., 2006. Modeling surface and ground water mixing in the hyporheic zone using MODFLOW and MT3D. Advances in Water Resources 29 (11), 1618−1633.

Liu, T., Xia, X., Liu, S., Mou, X., Qiu, Y., 2013. Acceleration of denitrification in turbid rivers due to denitrification occurring on suspended sediment in oxic waters. Environmental Science and Technology 47 (9), 4053−4061. https://doi.org/10.1021/es304504m.

Magliozzi, C., Grabowski, R.C., Packman, A.I., Krause, S., 2018. Toward a conceptual framework of hyporheic exchange across spatial scales. Hydrology and Earth System Sciences 22 (12), 6163−6185. https://doi.org/10.5194/hess-22-6163-2018.

Malard, F., Tockner, K., Dole-Olivier, M.-J.J., Ward, J.V., 2002. A landscape perspective of surface−subsurface hydrological exchanges in river corridors. Freshwater Biology 47 (4), 621−640. https://doi.org/10.1046/j.1365-2427.2002.00906.x.

Malcolm, I.A., Soulsby, C., Youngson, A.F., Hannah, D.M., 2005. Catchment-scale controls on groundwater-surface water interactions in the hyporheic zone: implications for salmon embryo survival. River Research and Applications 21, 977−989.

Marion, A., Bellinello, M., Guymer, I., Packman, A.I., 2002. Effect of bed form geometry on the penetration of nonreactive solutes into a streambed. Water Resources Research 38 (10), 1209.

Marion, A., Packman, A.I., Zaramella, M., Bottacin-Busolin, A., 2008a. Hyporheic flows in stratified beds. Water Resources Research 44, W09433.

Marion, A., Zaramella, M., Bottacin-Busolin, A., 2008b. Solute transport in rivers with multiple storage zones: the STIR model. Water Resources Research 44, W10406.

Marzadri, A., Bellin, A., Tank, J.L., Tonina, D., 2022. Predicting nitrous oxide emissions through riverine networks. Science of The Total Environment 843, 156844. https://doi.org/10.1016/j.scitotenv.2022.156844.

Marzadri, A., Dee, M.M., Tonina, D., Bellin, A., Tank, J.L., 2014. A hydrologic model demonstrates nitrous oxide emissions depend on streambed morphology. Geophysical Research Letters 41 (15), 5484–5491. https://doi.org/10.1002/2014GL060732.

Marzadri, A., Dee, M.M., Tonina, D., Bellin, A., Tank, J.L., 2017. Role of surface and subsurface processes in scaling N_2O emissions along riverine networks. Proceedings of the National Academy of Sciences 114 (17), 4330–4335. https://doi.org/10.1073/pnas.1617454114.

Marzadri, A., Tonina, D., Bellin, A., 2011. A semianalytical three-dimensional process-based model for hyporheic nitrogen dynamics in gravel bed rivers. Water Resources Research 47 (11), W11518. https://doi.org/10.1029/2011WR010583.

Marzadri, A., Tonina, D., Bellin, A., 2012. Morphodynamic controls on redox conditions and on nitrogen dynamics within the hyporheic zone: application to gravel bed rivers with alternate-bar morphology. Journal of Geophysical Research: Biogeosciences 117 (3). https://doi.org/10.1029/2012JG001966.

Marzadri, A., Tonina, D., Bellin, A., 2013a. Effects of stream morphodynamics on hyporheic zone thermal regime. Water Resources Research 49 (4), 2287–2302. https://doi.org/10.1002/wrcr.20199.

Marzadri, A., Tonina, D., Bellin, A., 2013b. Quantifying the importance of daily stream water temperature fluctuations on the hyporheic thermal regime: implication for dissolved oxygen dynamics. Journal of Hydrology 507, 241–248. https://doi.org/10.1016/j.jhydrol.2013.10.030.

Marzadri, A., Tonina, D., Bellin, A., 2020. Power law scaling model predicts N_2O emissions along the Upper Mississippi River basin. Science of the Total Environment 732, 138390. https://doi.org/10.1016/j.scitotenv.2020.138390.

Marzadri, A., Tonina, D., Bellin, A., Valli, A., 2016. Mixing interfaces, fluxes, residence times and redox conditions of the hyporheic zones induced by dune-like bedforms and ambient groundwater flow. Advances in Water Resources 88, 139–151. https://doi.org/10.1016/j.advwatres.2015.12.014.

Marzadri, A., Tonina, D., Bellin, A., Vignoli, G., Tubino, M., 2010. Semianalytical analysis of hyporheic flow induced by alternate bars. Water Resources Research 46 (7), W07531. https://doi.org/10.1029/2009WR008285.

Marzadri, A., Amatulli, G., Tonina, D., Bellin, A., Shen, L.Q., Allen, G.H., Raymond, P.A., 2021. Global riverine nitrous oxide emissions: the role of small streams and large rivers. Science of the Total Environment 776, 145148. https://doi.org/10.1016/j.scitotenv.2021.145148.

Master, Y., Shavit, U., Shaviv, A., 2005. Modified isotope pairing technique to study N transformations in polluted aquatic systems: theory. Environmental Science and Technology 39, 1749–1756.

Mendoza, C., Zhou, D., 1992. Effects of porous bed on turbulent stream flow above bed. Journal of Hydraulic Engineering 118 (9), 1222–1240.

Middleton, G.V., Southard, J.B., 1984. Mechanics of Sediment Movement. Society for Economic Paleontologists and Mineralogists Short Course No. 3, Tulsa, OK.

Monofy, A., Boano, F., 2021. The effect of streamflow, ambient groundwater, and sediment anisotropy on hyporheic zone characteristics in alternate bars. Water Resources Research 57, 1–22. https://doi.org/10.1029/2019WR025069.

Montgomery, D.R., Buffington, J.M., 1997. Channel-reach morphology in mountain drainage basins. Geological Society of America Bulletin 109, 596–611.

Montgomery, D.R., Buffington, J.M., 1998. Channel processes, classification, and response. In: Naiman, R.J., Bilby, R. (Eds.), River Ecology and Management. Springer-Verlag, New York, NY, pp. 13–42.

Moreto, J.R., Reeder, W.J., Budwig, R., Tonina, D., Liu, X., 2022. Experimentally mapping water surface elevation, velocity, and pressure fields of an open channel flow around a stalk. Geophysical Research Letters 49 (7), 1–10. https://doi.org/10.1029/2021gl096835.

Mrokowska, M.M., Osuch, M., 2011. Assessing validity of the dead zone model to characterize transport of contaminants in the River Wkra. In: Rowinski, P. (Ed.), Experimental Methods in Hydraulic Research, Geoplanet: Earth and Planetary Sciences, vol 1. Springer, Berlin, Heidelberg, pp. 235–246.

Mulholland, P.J., Helton, A.M., Poole, G.C., Hall, R.O., Hamilton, S.K., Peterson, B.J., Tank, J.L., Ashkenas, L.R., Cooper, L.W., Dahm, C.N., et al., 2008. Stream denitrification across biomes and its response to anthropogenic nitrate loading. Nature 452 (7184), 202–205. https://doi.org/10.1038/nature06686.

Mulholland, P.J., Marzorf, E.R., Webster, J.R., Hart, D.D., Hendricks, S.P., 1997. Evidence that hyporheic zones increase heterotrophic metabolism and phosphorus uptake in forest streams. Limnology & Oceanography 42, 443−451.

Naegeli, M.W., Uehlinger, U., 1997. Contribution of the hyporheic zone to ecosystem metabolism in a prealpine gravel-bed-river. Journal of the North American Benthological Society 16 (4), 794−804.

Nagaoka, H., Ohgaki, S., 1990. Mass transfer mechanism in a porous riverbed. Water Research 24 (4), 417−425.

Ocampo, C.J., Oldham, C.E., Sivapalan, M., 2006. Nitrate attenuation in agricultural catchments: shifting balances between transport and reaction. Water Resources Research 42 (W01408), 16.

Orghidan, T., 1959. Ein neuer lebensraum des unterirdischen wassers: der hyporheische biotop. Archiv für Hydrobiologie 55, 392−414.

Packman, A.I., Brooks, N.H., 2001. Hyporheic exchange of solutes and colloids with moving bed forms. Water Resources Research 37 (10), 2591−2605. https://doi.org/10.1029/2001WR000477.

Packman, A.I., Brooks, N.H., Morgan, J.J., 2000. A physicochemical model for colloid exchange between a stream and a sand streambed with bed forms. Water Resources Research 36 (8), 2351−2361.

Pescimoro, E., Boano, F., Sawyer, A.H., Soltanian, M.R., 2019. Modeling influence of sediment heterogeneity on nutrient cycling in streambeds. Water Resources Research 55 (5), 4082−4095. https://doi.org/10.1029/2018WR024221.

Poole, G.C., O'Daniel, S.J., Jones, K.L., Woessner, W.W., Bernhardt, E.S., Helton, A.M., Stanford, J.A., Boer, B.R., Beechie, T.J., 2008. Hydrologic spiralling: the role of multiple interactive flow paths in stream ecosystems. River Research and Applications 24, 1018−1031.

Pryshlak, T.T., Sawyer, A.H., Stonedahl, S.H., Soltanian, M.R., 2015. Multiscale hyporheic exchange through strongly heterogeneous sediments. Water Resources Research 51 (11), 9127−9140.

Quick, A.M., Reeder, W.J., Farrell, T.B., Tonina, D., Feris, K.P., Benner, S.G., 2016. Controls on nitrous oxide emissions from the hyporheic zones of streams. Environmental Science and Technology 50 (21), 11491−11500. https://doi.org/10.1021/acs.est.6b02680.

Raymond, P.A., Zappa, C.J., Butman, D., Bott, T.L., Potter, J., Mulholland, P.J., Laursen, A.E., McDowell, W.H., Newbold, D., 2012. Scaling the gas transfer velocity and hydraulic geometry in streams and small rivers. Limnology & Oceanography 2 (1), 41−53. https://doi.org/10.1215/21573689-1597669.

Reeder, W.J., Quick, A.M., Farrell, T.B., Benner, S.G., Feris, K.P., Basham, W.J.R., Marzadri, A., Tonina, D., Huber, C., 2019. A novel fiber optic system to map dissolved oxygen concentrations continuously within submerged sediments. Journal of Applied Water Engineering and Research 7 (3), 1−12. https://doi.org/10.1080/23249676.2019.1611495.

Reeder, W.J., Quick, A.M., Farrell, T.B., Benner, S.G., Feris, K.P., Marzadri, A., Tonina, D., 2018a. Hyporheic source and sink of nitrous oxide. Water Resources Research 54 (7), 5001−5016. https://doi.org/10.1029/2018WR022564.

Reeder, W.J., Quick, A.M., Farrell, T.B., Benner, S.G., Feris, K.P., Tonina, D., 2018b. Spatial and temporal dynamics of dissolved oxygen concentrations and bioactivity in the hyporheic zone. Water Resources Research 54 (3), 2112−2128. https://doi.org/10.1002/2017WR021388.

Reisinger, A.J., Tank, J.L., Rosi-Marshall, E.J., Hall, R.O., Baker, M.A., 2015. The varying role of water column nutrient uptake along river continua in contrasting landscapes. Biogeochemistry 125 (1), 115−131. https://doi.org/10.1007/s10533-015-0118-z.

Ren, J., Packman, A.I., 2004a. Modeling of simultaneous exchange of colloids and sorbing contaminants between streams and streambeds. Environmental Science and Technology 38 (10), 2901−2911.

Ren, J., Packman, A.I., 2004b. Coupled stream-subsurface exchange of colloidal hematite and dissolved zinc, copper and phosphate. Environmental Science and Technology 39 (17), 6387−6394.

Ren, J., Packman, A.I., 2007. Changes in fine sediment size distributions due to interactions with streambed sediments. Sedimentary Geology 202, 529−537.

Ritzi, R.W., Dai, Z., Dominic, D.F., Rubin, Y.N., 2004. Spatial correlation of permeability in cross-stratified sediment with hierarchical architecture. Water Resources Research 40, W03513.

Riva, M., Guadagnini, L., Guadagnini, A., Ptak, T., Martac, E., 2006. Probabilistic study of well capture zones distribution at the Lauswiesen field site. Journal of Contaminant Hydrology 88 (1), 92−118.

Roche, K.R., Li, A., Bolster, D., Wagner, G.J., Packman, A.I., 2019. Effects of turbulent hyporheic mixing on reach-scale transport. Water Resources Research 55 (5), 3780−3795. https://doi.org/10.1029/2018WR023421.

Rousseau, G., Ancey, C., 2020. Scanning PIV of turbulent flows over and through rough porous beds using refractive index matching. Experiments in Fluids 61 (8), 1–24. https://doi.org/10.1007/s00348-020-02990-y.

Rubol, S., Tonina, D., Vincent, L., Sohm, J.A., Basham, W., Budwig, R., Savalia, P., Kanso, E., Capone, D.G., Nealson, K.H., 2018. Seeing through porous media: an experimental study for unveiling interstitial flows. Hydrological Processes 32 (3), 402–407. https://doi.org/10.1002/hyp.11425.

Runkel, R.L., 1998. One-dimensional Transport with Inflow and Storage (OTIS): A Solute Transport Model for Streams and Rivers. US Geological Survey, Water-Resources Investigations Report 98-4018, Denver, CO.

Salarashayeri, A.F., Siosemarde, M., 2012. Prediction of soil hydraulic conductivity from particle-size distribution. International Journal of Geological and Environmental Engineering 61, 454–458.

Salehin, M., Packman, A.I., Paradis, M., 2004. Hyporheic exchange with heterogeneous streambeds: laboratory experiments and modeling. Water Resources Research 40 (11), W11504.

Sawyer, A.H., Cardenas, M.B., 2009. Hyporheic flow and residence time distributions in heterogeneous cross-bedded sediment. Water Resources Research 45, W08406.

Sawyer, A.H., Cardenas, M.B., Buttles, J., 2011. Hyporheic exchange due to channel-spanning logs. Water Resources Research 47, W08502.

Sheibley, R.W., Jackman, A.P., Duff, J.H., Triska, F.J., 2003. Numerical modeling of coupled nitrification–denitrification in sediment perfusion cores from the hyporheic zone of the Shingobee River, MN. Advances in Water Resources 26, 977–987.

Shen, H.V., Fehlman, H.M., Mendoza, C., 1990. Bed form resistance in open channel flows. Journal of Hydraulic Engineering 116 (6), 799–815.

Shen, G., Yuan, J., Phanikumar, M.S., 2020. Direct numerical simulations of turbulence and hyporheic mixing near sediment-water interfaces. Journal of Fluid Mechanics 892 (A20). https://doi.org/10.1017/jfm.2020.173.

Sherman, T., Roche, K.R., Richter, D.H., Packman, A.I., Bolster, D., 2019. A dual domain stochastic Lagrangian model for predicting transport in open channels with hyporheic exchange. Advances in Water Resources 125, 57–67. https://doi.org/10.1016/j.advwatres.2019.01.007.

Singh, T., Gomez-Velez, J.D., Wu, L., Wörman, A., Hannah, D.M., Krause, S., 2020. Effects of successive peak flow events on hyporheic exchange and residence times. Water Resources Research 56 (8), e2020WR027113. https://doi.org/10.1029/2020WR027113.

Stanford, J.A., 2006. Landscapes and riverscapes. In: Hauer, F.R., Lamberti, G.A. (Eds.), Methods in Stream Ecology. Academic Press, San Diego, CA, pp. 3–21.

Stanford, J.A., Ward, J.V., 1993. An ecosystem perspective of alluvial rivers: connectivity and the hyporheic corridor. Journal of the North American Benthological Society 12 (1), 48–60.

Stanford, J.A., Lorang, M.S., Hauer, F.R., 2005. The shifting habitat mosaic of river ecosystems. Verhandlungen Internationale Vereinigung für Theoretische und Angewandte Limnologie 29 (1), 123–136. https://doi.org/10.1080/03680770.2005.11901979.

Stewart, R.J., Wollheim, W.M., Gooseff, M.N., Briggs, M.A., Jacobs, J.M., Peterson, B.J., Hopkinson, C.S., 2011. Separation of river network–scale nitrogen removal among the main channel and two transient storage compartments. Water Resources Research 47, W00J10.

Stonedahl, S.H., Harvey, J.W., Packman, A.I., 2013. Interaction between hyporheic flow produced by stream meanders, bars and dunes. Water Resources Research 49, 5450–5461.

Stonedahl, S.H., Harvey, J.W., Wörman, A., Salehin, M., Packman, A.I., 2010. A multi-scale model for integrating hyporheic exchange from ripples to meanders. Water Resources Research 46, W12539.

Storey, R.G., Howard, K.W.F., Williams, D.D., 2003. Factor controlling riffle-scale hyporheic exchange flows and their seasonal changes in gaining stream: a three-dimensional groundwater model. Water Resources Research 39 (2), 1034. https://doi.org/10.1029/2002WR001367.

Stuart, T.A., 1954. Spawning sites of trout. Nature 173, 354.

Thibodeaux, L.J., Boyle, J.D., 1987. Bedform-generated convective transport in bottom sediment. Nature 325 (22), 341–343.

Tonina, D., 2012. Surface water and streambed sediment interaction: the hyporheic exchange. In: Gualtieri, C., Mihailovic, D.T. (Eds.), Fluid Mechanics of Environmental Interfaces. CRC Press, Taylor and Francis Group, London, pp. 255–294.

Tonina, D., Buffington, J.M., 2007. Hyporheic exchange in gravel bed rivers with pool-riffle morphology: laboratory experiments and three-dimensional modeling. Water Resources Research 43, W01421. https://doi.org/10.1029/2005WR004328.

Tonina, D., Buffington, J.M., 2009. Hyporheic exchange in mountain rivers I: mechanics and environmental effects. Geography Compass 3 (3), 1063–1086. https://doi.org/10.1111/j.1749-8198.2009.00226.x.

Tonina, D., Buffington, J.M., 2011. Effects of stream discharge, alluvial depth and bar amplitude on hyporheic flow in pool-riffle channels. Water Resources Research 47 (8), W08508. https://doi.org/10.1029/2010WR009140.

Tonina, D., de Barros, F.P.J., Marzadri, A., Bellin, A., 2016. Does streambed heterogeneity matter for hyporheic residence time distribution in sand-bedded streams? Advances in Water Resources 96, 120–126. https://doi.org/10.1016/j.advwatres.2016.07.009.

Tonina, D., Marzadri, A., Bellin, A., 2015. Benthic uptake rate due to hyporheic exchange: the effects of streambed morphology for constant and sinusoidally varying nutrient loads. Water (Switzerland) 7 (2), 398–419. https://doi.org/10.3390/w7020398.

Trauth, N., Schmidt, C., Maier, U., Vieweg, M., Fleckenstein, J.H., 2013. Coupled 3-D stream flow and hyporheic flow model under varying stream and ambient groundwater flow conditions in a pool-riffle system. Water Resources Research 49 (9), 5834–5850. https://doi.org/10.1002/wrcr.20442.

Trauth, N., Schmidt, J.C., Vieweg, M., Maier, U., Fleckenstein, J.H., 2014. Hyporheic transport and biogeochemical reactions in pool-riffle systems under varying ambient groundwater flow conditions. Journal of Geophysical Research: Biogeosciences 119, 910–928.

Triska, F.J., Duff, J.H., Avanzino, R.J., 1993. Patterns of hydrological exchange and nutrient transformation in the hyporheic zone of a gravel bottom stream: examining terrestrial-aquatic linkages. Freshwater Biology 29, 259–274.

Triska, F.J., Kennedy, V.C., Avanzino, R.J., Zellweger, G.W., Bencala, K.E., 1989a. Retention and transport of nutrients in a third-order stream: channel processes. Ecology 70, 1894–1905.

Triska, F.J., Kennedy, V.C., Avanzino, R.J., Zellweger, G.W., Bencala, K.E., 1989b. Retention and transport of nutrients in a third-order stream in Northwestern California: hyporheic processes. Ecology 70 (6), 1893–1905.

Tubino, M., 1991. Growth of alternate bars in unsteady flow. Water Resources Research 27 (1), 37–52.

van Kampen, R., Schneidewind, U., Anibas, C., Bertagnoli, A., Tonina, D., Vandersteen, G., Luce, C., Krause, S., van Berkel, M., 2022. LPMLE*n*–A frequency domain method to estimate vertical streambed fluxes and sediment thermal properties in semi-infinite and bounded domains. Water Resources Research 58 (3), e2021WR030886. https://doi.org/10.1029/2021WR030886.

Vaux, W.G., 1968. Intragravel flow and interchange of water in a streambed. Fishery Bulletin 66 (3), 479–489.

Vieweg, M., Trauth, N., Fleckenstein, J.H., Schmidt, C., 2013. Robust optode-based method for measuring in situ oxygen profiles in gravelly streambeds. Environmental Science & Technology 47 (17), 9858–9865. https://doi.org/10.1021/es401040w.

Vittal, N., Ranga Raju, K.G., Garde, R.J., 1977. Resistance of two-dimensional triangular roughness. Journal of Hydraulic Research 15 (1), 19–36.

Voermans, J.J., Ghisalberti, M., & Ivey, G.N., 2018. The hydrodynamic response of the sediment-water interface to coherent turbulent motions. Geophysical Research Letters 45(19), 10,520–10,527. https://doi.org/10.1029/2018GL079850

Ward, A.S., Gooseff, M.N., Johnson, P.A., 2011. How can subsurface modifications to hydraulic conductivity be designed as stream restoration structures? Analysis of Vaux's conceptual models to enhance hyporheic exchange. Water Resources Research 47 (8), W09418.

Ward, A.S., Gooseff, M.N., Singha, K., 2010. Imaging hyporheic zone solute transport using electrical resistivity. Hydrological Processes 24, 948–953.

White, D.S., 1993. Perspective on defining and delineating hyporheic zones. Journal of the North American Benthological Society 12 (1), 61–69.

Winter, C.L., Tartakovsky, D.M., 2002. Groundwater flow in heterogeneous composite aquifers. Water Resources Research 38 (8).

Winter, T.C., Harvey, J.W., Franke, O.L., Alley, W.M., 1998. Ground Water and Surface Water: A Single Resource. U.S. Geological Survey, Circular 1139, Denver, CO.

Wolke, P., Teitelbaum, Y., Deng, C., Lewandowski, J., Arnon, S., 2019. Impact of bed form celerity on oxygen dynamics in the hyporheic zone. Water 12 (1), 62. https://doi.org/10.3390/w12010062.

Wondzell, S.M., 2011. The role of the hyporheic zone across stream networks. Hydrological Processes 25 (22), 3525–3532.

Wondzell, S.M., Gooseff, M.N., 2013. Geomorphic controls on hyporheic exchange across scales: watersheds to particles. In: Shroder (Ed.-in-chief), J.F., Wohl (vol. Ed.), E. (Eds.), Treatise on Geomorphology, 9. Fluvial Geomorphology. Academic Press, San Diego, CA, pp. 203–218. Fluvial Geomorphology.

Wondzell, S.M., Swanson, F.J., 1996. Seasonal and storm dynamics of the hyporheic zone of a 4th order mountain stream. 1: hydrologic processes. Journal of the North American Benthological Society 15, 3–19.

Wörman, A., Packman, A.I., Johansson, H., Jonsson, K., 2002. Effect of flow-induced exchange in hyporheic zones on longitudinal transport of solutes in streams and rivers. Water Resources Research 38 (1), 2–15.

Wörman, A., Packman, A.I., Marklund, L., Harvey, J.W., 2006. Exact three-dimensional spectral solution to surface-groundwater interaction with arbitrary surface topography. Geophysical Research Letters 33, L07402.

Wu, L., Gomez-Velez, J.D., Krause, S., Singh, T., Wörman, A., Lewandowski, J., 2020. Impact of flow alteration and temperature variability on hyporheic exchange. Water Resources Research 56 (3), e2019WR026225. https://doi.org/10.1029/2019wr026225.

Wuhrmann, K., 1972. River purification. In: Mitchell, R. (Ed.), Water Pollution Microbiology. Wiley-Interscience, New York, NY, pp. 119–151.

Xia, X., Yang, Z., Zhang, X., 2009. Effect of suspended-sediment concentration on nitrification in river water: importance of suspended sediment − water interface. Environmental Science and Technology 43 (10), 3681–3687. https://doi.org/10.1021/es8036675.

Yalin, M.S., 1964. Geometrical properties of sand waves. Journal of the Hydraulics Division 90, 105–119.

Yuan, Y, Chen, X., Cardenas, M.B., Liu, X., Chen, L., 2021. Hyporheic exchange driven by submerged rigid vegetation: a modeling study. Water Resources Research 57 (6), e2019WR026675. https://doi.org/10.1029/2019WR026675.

Zaramella, M., Packman, A.I., Marion, A., 2003. Application of the transient storage model to analyze advective hyporheic exchange with deep and shallow sediment beds. Water Resources Research 39 (7), 1198.

Zarnetske, J.P., Gooseff, M.N., Bowden Morgan, J., Greenwald, M.J., Brosten, T.R., Bradford, J.H., McNamara, J.P., 2008. Influence of morphology and permafrost dynamics on hyporheic exchange in arctic headwater streams under warming climate conditions. Geophysical Research Letters 35, L02501.

Zarnetske, J.P., Haggerty, R., Wondzell, S.M., Baker, M.A., 2011. Dynamics of nitrate production and removal as a function of residence time in the hyporheic zone. Journal of Geophysical Research: Biogeosciences 116, G01025.

Zarnetske, J.P., Haggerty, R., Wondzell, S.M., Bokil, V.A., González-Pinzón, R., 2012. Coupled transport and reaction kinetics control the nitrate source-sink function of hyporheic zones. Water Resources Research 48, W11508.

Zhou, Y., Ritzi, R.W., Soltanian, M.R., Dominic, D.F., 2014. The influence of streambed heterogeneity on hyporheic flow in gravelly rivers. Ground Water 52 (2), 206–216.

Ziebis, W., Forster, S., Huettel, M., Jørgensen, B.B., Jorgensen, B.B., 1996. Complex burrows of mud shrimp *Callianassa truncata* and their geochemical impact in the sea bed. Nature 382 (6592), 619–622.